Response to Anonymous Reviewer #1
We thank the reviewer for his work and the valuable comments. We are convinced that addressing the issues raised by the reviewer considerably improved the manuscript. Please see our reply below.

Note:
Reviewer comments are in italics.
Author responses are in normal format.
Changes that were made to the manuscript are in **bold** face with examples of the new text in blue.

1. The authors state that resonant ionization of metals in single particles is becoming independent of the particle matrix and its atmospheric changes. This is an important point, however, there is not enough evidence to support it. Although the enhancement effect has been observed not only in Fe-rich but also in other Fe-containing particles, it doesn't mean that the particle matrix won't play a role. I would argue that the degree of enhancement may change in different particle types. This is actually shown in Fig 2: when comparing the wavelength at 248. 3 and ~247 nm, an enhancement of the Fe-54 signal is above 2 and below 2 for diesel soot and Arizona test dust, respectively. Please add more discussions, rephrase the abstract and the conclusion sections.

We agree that the matrix still plays a role, especially during heating and desorption within the leading edge of the laser pulse and before the resonance with free atoms becomes effective. In our ambient air experiment, where the same particle ensemble was probed with two different wavelengths, we see that Fe-detection was restricted to a particular matrix (EC) in non-resonant LDI, which is in line with other studies that the strongly absorbing soot components augment ionization (e.g. Zimmermann et al., 2003). For resonant LDI, also particles without EC signature, but OC and even strong sea salt contribution revealed Fe. Reinard et al. (2008) showed that energetically preferred ions survive and thus dominate the spectrum, which explains the substantial fraction of the matrix effect that results from charge transfer in the plume. This is in line with our explanation, that strong light absorption enhances the degree of ionization for Fe which can therefore be detected even if high abundances of e.g. Na+ and K+ ions are in the plume.

changes made to the manuscript:
Following the reviewer's comment, we rephrased the discussion on matrix effects throughout the manuscript and avoid the term "matrix effect" for our discussion.

- **abstract: statement on dependency on the matrix effect removed. New sentence:**
  "Many of the particles that showed iron contents upon resonant LDI were mixtures of sea salt and organic carbon. For non-resonant ionization, iron was exclusively detected in particles with a soot contribution. This suggests that resonant LDI allows a more universal and secure metal detection in SPMS."
- **caption Fig. 5: statement on matrix effect dependency removed.**
- **Discussion of ambient air experiment. Sentence on matrix effects as well as comparison to REMPI and quantification removed.**

2. Experimental Section (consider to change the header to "Methods")
1) This study focused on both technical improvements and application, thus more description of the instrument should be added, even though it has been described in other publications. The following points should be addressed in the main manuscript and/or supporting information. Briefly describe the inlet system (inlet type? transmission efficiency of the inlet to standard samples, e.g., PSL?), particle detection region (what is the detection limit of particle size? Scattering efficiency?), LDI region (hit rate for ArF and KrF?), spectra generation (e.g., some descriptions of data analysis in section 3.3 should be moved to the method section), and what is the overall transmission efficiency/detection efficiency of this instrument to PSL particles or other standard samples? In the field measurement, a custom electronic circuit was applied to trigger the lasers alternately. What is the firing time for each one?

changes made to the manuscript:
We added the requested technical information, further references and re-structured the "Methods" section accordingly.

- **example on new text on the basic instrumental design**
  "Briefly, its instrumental layout is conceptually close to the ATOF-MS (Su et al., 2004) with an aerodynamic lens inlet and an optical sizing unit that comprises of a pair of 75 mW cw-lasers at a wavelength of 532 nm, ellipsoidal mirrors and photomultipliers. The dual-polarity mass spectrometer is

designed in Z-TOF geometry, as introduced by (Pratt et al., 2009). For further details, e.g. the inlet particle transmission and detection efficiency, we refer to the literature (Li et al., 2011; Zhou et al., 2016). After the laboratory experiments, we implemented delayed ion extraction (Δt=0.4 µs) using high-voltage switches (HTS31-03-GSM, Behlke GmbH, Germany) to improve the peak quality in the ambient air experiments (Vera et al., 2005; Li et al., 2018)"

- The hit rates for the ArF and KrF lasers are shown in Fig. 5.
- **on the electronics and firing time:** "The two KrF and ArF excimer lasers used in this experiment were alternately triggered to particles using a custom electronic circuit based on a complex programmable logic device (Intel Max V) with 8.5 ns pin-to-pin delay and programmed using Very High Speed Integrated Circuit Hardware Description Language (VHDL)."

2) In the manuscript, "delayed ion extraction" was used and mentioned in section 3.3 Line 234, but not described in method section. Please add it at least in the supporting information.

Information added. See previous item.

3) Regarding surrogates. Why was the diesel soot chosen as the anthropogenic Fe-containing particles? I suggest that some standard samples with specific Fe signal, e.g., hematite, should also be measured. This allows to see 2 more prominent resonant enhancement and the ratio of Fe-56/Fe-54 can be determined, which could help to refine the enhancement effect for other particle types.

In our study, we focused on the practical implications of the resonance for ambient air applications, and thus we tried to choose realistic proxies for the most relevant aerosols. We also worked with different particle types such as hematite. Unfortunately, the Fe signal was too strong in Fe-rich aerosols such as hematite, which lead to massive saturation effects, as already mentioned for Arizona test dust. Even with reduced detector voltages, the dynamic range of our SPMS was not sufficient to achieve a good peak quality, while preserving neighboured signals of other ions. Following the advice of the referee, we tried further particle systems and had some success with hemoglobin powder. We added this results in the Supplement. There were no general differences to the diesel or dust particles and the resonance effect was also observed for hemoglobin.

changes made to the manuscript:
We performed new experiments with hematite and hemoglobin, added the results on hemoglobin in the Supplemental Fig. S4 and refer to it in the manuscript.

3. Results and discussion
1) The mass spectra are shown in an accumulated way, without normalization or further processing. However, the accumulation method is not able to reduce the shot-to-shot difference, which might bring big uncertainty to the results. As stated in the manuscript, the irregularly triggered OPO system reduced its pulse stability. In the ambient, more stable excimer lasers were used, but the ambient particles are more dispersed and complicated. Therefore, further processing is highly recommended. For individual particles, normalization to the total ion intensity can account for shot-to-shot variability (Hatch et al., 2014; Shen et al., 2018). Afterwards, averaging the normalized ones can give statistically more relevant results.

With the accumulated, unprocessed spectra, we intend to show the magnitude of the physical resonance effect, i.e. the increase of ion current. This information would be biased by normalization. We agree with the reviewer, that the increase in detection efficiency can better be depicted by the signal normalized to total ion signal of each particle. This is exactly what we did in the histograms, where the relative signal of ^{54}Fe normalized to total ion signal is shown, revealing the single-particle distribution of this signal and thus giving an impression of the detection frequency for Fe. We would prefer to avoid large additional mass spectra for normalized data in the manuscript and prepared those plots for the Supplement.

changes made to the manuscript:

- **We added normalized spectra for all model particles in the Supplement (Figs. S2-S5) and referred to in the manuscript.**

In order to further investigate the resonant enhancement, the authors measured the wavelength-dependent total ion yield of Fe-54 shown in Figure 2. It would be better to show the averaged relative ion yield with standard deviation, which may give an ion yield curve with less broadening.

Following the advice of the reviewer, we performed the experiment again and made 3 replicates with each 400 analysed particles for every wavelength. This allowed us to add standard deviation error bars.

Regarding the normalization, the argumentation is the same as for the previous issue. To account for the reviewer's comments, we prepared the same plots with the signal normalized to total ion counts and added it in the Supplemental.

changes made to the manuscript:

- **new data measured for diesel soot and Arizona dust**
- **numbers of analysed particles per wavelength increased from 400 to 1200**
- **error bars included**
- **new Figure 2**
- **new Figure S3 with normalized data.**

2) Bias induced by organics and uncertainty of the results should be discussed. For diesel soot, m/z 56+ could also originate from organics e.g., C4H8+. Similar interference effects could rise from m/z 56 CaO+ for Arizona Test Dust. Therefore, the enhancement of Fe signals could be underestimated (based on the results that KrF excimer laser leads to ionization enhancement of Fe, but does not change or even reduce the signals of organics). It would be great if this can be discussed more. M/z 54+ is a more characteristic peak for iron, but it is rather weak compared to m/z 56+. Such weak signals can be close to the noise level. As mentioned above, measurement of some standard samples like hematite may provide useful information for discussion.

According to the reviewer's advice, we extended the discussions on such interferences. We agree that these interferences might lead to an underestimation of the resonance effect, but it appears impossible to avoid it for realistic aerosols without substantially higher mass resolution. We prefer to leave the assessment of the effect strengths to the reader by providing the data in the figures, as this is quite difficult and differs across the particle types.
As mentioned before, we did additional experiments with other particles and added the hemoglobin results in the Supplement.

changes made to the manuscript:

- **Discussion on interferences and possible underestimation of the enhancement effect added and emphasised throughout the manuscript.**

  "Even stronger saturation effects producing highly corrupted Fe-peaks were observed for hematite, which is consequently not shown here. Because interferences with CaO^+ and organic fragments like $C_3H_4O^+$ can affect the signal differences at m/z=56, the histograms show the signal of the ^{54}Fe isotope. Contributions from organic fragments to m/z=54 are assumed to be rather small, as apparent from the signal strengths of principal fragments in the respective mass range at m/z=51, 53 and 55, see inset of Figure 1(a). However, such interferences might lead to a moderate underestimation of the resonance enhancement."
- **new data measured for hemoglobin and presented in Fig. S4 as mentioned before.**

3) In section 3.1 and Fig. 1. Why were wavelengths at 250 nm and 242.2 nm chosen to compare with 248.3 nm for diesel soot and Arizona test dust, respectively? Please clarify the reasons (242.2 was chosen to show the enhancement effect for Li?). Please consider to show more wavelengths (e.g., <248, 248, >248) for comparison and keep consistency for different samples. Similar questions and comments apply to section 3.3 and Fig. 3.

We thank the reviewer for his attentive look. Indeed, a reference wavelength at 242 nm was foreseen, the 250 nm reference is our mistake. We corrected the figure and text accordingly, that both for the soot and the dust the same wavelength are compared (apart from a small deviation of 0.3 nm related to the OPO/spectrometer inaccuracy). Now, in all spectra, the reference wavelength is shorter, i.e. the photon energy is higher. Thus, possible effects of a higher photon energy, e.g. photoionization thresholds, are excluded and the enhancement can be attributed to the resonance with a higher level of certainty. Only for Zn, the reference wavelength is longer, which is associated with the instrument's UV limit and explained in the text.
Moreover, we added new data, comparing the Fe, Mn and Zn yield between three wavelengths (below resonance, at res. and above res.), as suggested by the reviewer. Because such plots showing three spectra are quite complex, we added them in the Supplement. For soot and Arizona dust, an extensive wavelength comparison is shown in Figure 2.

changes made to the manuscript:

- **new Figure 1 now shows a consistent wavelength comparison for Diesel soot and Arizona dust.**
- **statement on the exception of a higher wavelength for Zn added in the text.**
- **new data shown in Supplemental Figure S5 presents three-wavelength comparison for all Fe, Mn and Zn in NIST urban dust.**

4. Atmospheric implications and conclusions should be strengthened. Consider to add an implication section or implement it to the conclusion section as it is now. However, several points should be addressed. For the conclusions, the authors should answer e.g., how much enhancement (%) can be achieved? What about the uncertainty? What are the weaknesses of the technique? E.g., resonant ionization enhancement can only be obtained for a few metals simultaneously. In addition, the sensitivity to the other species, e.g., organics, might be reduced while it is enhanced to metals. Hence, tuneable laser systems are required. For the implications consider mentioning that particle-bound metals, such as iron, can also serve as catalyst or reactant in chemistry. Consider to add more discussions on how this study can help understand/investigate the role of particle-bound metal and/or metal oxides in atmospheric processes, e.g., heterogeneous chemistry, transportation, etc. 3

We thank the reviewer for considering our results generally important and the suggestions. We added a new discussion part to the ambient air results, focusing on the Fe-content of salt and organic aerosols we observed. We discuss these results in the context of previous SPMS studies. Moreover we extended the discussion and conclusions on atmospheric implications as suggested by the reviewer.

changes made to the manuscript:

- **new part discussing the mixing state of Fe-containing particles and implications for future studies. Additional text and references.**

"Although our field study provides only a limited dataset, some general implications can already be derived. The internal mixing of Fe with sulfate or organic acids is assumed to be crucial for Fe dissolution, and thus for the anthropogenic increase of bioavailable iron input to the oceans (Li et al., 2017). Previous studies indicated that the Fe transport into the sea is dominated by coal combustion particles containing sulfate in Asia (Furutani et al., 2011; Moffet et al., 2012), while the majority of Fe-containing particles in Europe are mixed with nitrate and were attributed to traffic activities (Dall'Osto et al., 2016). Similar to our experiment, these studies found strong internal mixing of many Fe-containing particles, such as biomass burning signals with coal combustion contributions in Asia and secondary nitrate with Fe in Europe. However, Fe-particles with sea-salt signatures were negligible in the SPMS studies and mixtures of Fe and OC were a minor fraction (Furutani et al., 2011; Dall'Osto et al., 2016). In our study, these particles were the most abundant types of Fe-containing particles, if resonant ionization was applied, see Fig 5(b), while for non-resonant ionization, particles with EC signatures were dominant (Fig. 5(a)). Taking into account that the aforementioned SPMS studies utilized non-resonant LDI of Fe at 266 nm, Fe-transport in organic and salt/mixed aerosols might have been underestimated. Electron microscopy studies of individual particles in Asia frequently revealed thick coatings of secondary compounds and organic matter around Fe-rich particle components (Li et al., 2017; Moffet et al., 2012). Ultra-fine Fe-containing particles, such as soot from traffic emissions, can enter the long-range transported accumulation mode via agglomeration with larger particles and condensation of organic vapours, secondary nitrate or sulfate. In our study, we observed a high prevalence of Fe in sea salt and OC particle types, indicating the importance of these pathways for transport of biologically relevant Fe."

- **Conclusion section extended to better address the general implications for atmospheric chemistry.**

"Not all physical details are fully understood, and the signal enhancement effects providing the basis for the improved metal detection efficiency are difficult to quantify for the different particle types. However, our results show that the increase in sensitivity is moderate for particular Fe-rich aerosols, such as the about 3-fold signal enhancement for Arizona test dust. The resonance enhancement appears to become more effective for mixed particles with smaller Fe-contributions such as in the ambient air experiment, where about 10 times more particles revealed Fe-signatures in direct comparison with non-resonant ionization. Taking into account the lower hit rate of the KrF laser, a downside related to its lower photon energy, the overall efficiency to identify Fe signatures in a single-particle mass spectrum was increased by a factor of about 20 in our ambient air study.

The coincidental matching of the KrF laser line with a strong absorption of Fe atoms allows an easy and straightforward application of the resonance effect in the field. For direct comparison of KrF with ArF lasers, it has to be considered that the lower photon energy of KrF laser is associated with a reduced hit rate and different mass spectral signatures of other particle components, e.g. organics. Further studies are required to evaluate these differences. Of note, because of its rather high pulse energy and the flat-top beam profile, the hit rate of the KrF laser was about 40−50 % in our experiment, which is still more than the values that are typically achieved with the most common laser line in SPMS, the Nd:YAG at 266 nm. Exploiting the resonance effect for other metals than Fe requires a tuneable Nd:YAG-OPO system, which is, however, more difficult to operate."

Minor comments
Page(P) 3 Line (L)64: Regarding typical ionization products, metals especially alkaline metals (e.g., Na, K) and mineral components such as silicate should be mentioned.

changed accordingly

P3L65: Change "EC, OC" to "EC or OC".

corrected

P3L66: Why is it "unique" compared to the other kinds of source information?

"unique" should emphasise the combination of single-particle information and metal detection. Changed "Beyond" to "Along with". Added examples for source apportionment using metal signatures.

P3L75: "Herein" would mislead the reader to think that the two-step technique was used in this study. However, one step LDI was used.

corrected

P4L101: What does "meaningful" mean? Please describe.

"Meaningful" removed, conditions described.

P4L106: "0-3 µm" change the short line to a long one "–" and mention the diameter type (physical?).

This is the official name of the dust, we added "diameter", since we could not find the information to which diameter type the name refers, most probably geometrical diameter.

P4L107: "modelled" might cause ambiguity. Consider another word, e.g., mimic.

changed accordingly

P4L112–115: Is the concentration factor (=3000?) stable? What was the upstream particle number concentration to the inlet of the instrument? What were the particle number and mass concentrations during the measurement time?

The real concentration factor is most probably lower than 3000, but difficult to measure for an ambient air ensemble, since the complete sampling line as well as the particle inlet have to be modified for a comparison.

changes made to the manuscript:

- **To provide an estimate on the concentration, we added two size distributions in the Supplemental Fig. S1, one with concentrator and one without. These were measured on ambient aerosols at the same site, but at a different day.**
- **Moreover, we added mean PM2.5 and PM1 mass concentrations to the manuscript. These were measured at the meteorological station with standard instrumentation during our ambient air experiment.**

P5L120: Table1 Change "x" to multiplication sign "×". Change "…" to "to" or "–" and throughout the manuscript.

corrected

P5L127: Aren't those accumulated spectra rather than averaged ones? I am confused here.

changed "averaged" to accumulated

P6L132: "much stronger Fe-signals". Please quantify such enhancement. How much % stronger?

The enhancement is quantified a bit later in the text. We would prefer to guide the reader's attention to the spectrum here.

P6L141: In the histogram plots of Fig.1, what is the difference between the light red and dark red? Please add descriptions in the figure caption as well. Similar comment is applied to Fig. 3.

The bars are transparent, and the dark areas are the overlapping areas. We prepared high-quality figures for publication, where these differences will be clearly visible.

P6L147: This is the first time to mention supporting information, thus it should be Fig. S1 rather than S4. Please revise accordingly throughout the manuscript.

Corrected. We re-organized the Supplement.

P7L151: Such signal enhancement of 4 is compared to which value at which wavelength? As shown in Fig2, when compared to the lowest value, they are 7 for diesel soot and 4 for mineral dust; comparing the wavelength at 248. 3 and ~247 nm, an enhancement of Fe-54 signal is >2 and <2 for diesel soot and Arizona test dust, respectively.

Because a clear baseline for a minimum yield does not exist (e.g. because also resonances with other lines occur, see Fig. 2), the effect can hardly be quantified with the few wavelength points we could address in these difficult and time-consuming experiments. We therefore estimated a conservative value of 3-4 from the lowest points to the maxima in Fig. 2.

P7L155–160: Change this sentence to "Thomson et al. (1997) observed ….bulk material." Similarly, please revise the sentence "Wade et al…".

corrected

P7L158: Give the full name of "MALDI".

corrected

P7L160: Add reference.

We cannot identify the issue. There are three references for this statement.

P7L164: Fig. 2 please use the same scale for OPO wavelength in panel (a) and (b). Add Y axis with the corresponding units for atomic absorption spectrum and for KrF laser spectrum.

changes made to the manuscript:

- **Fig. 2 is a complete new version showing new data and with the same OPO wavelength scale.**
- **The values measured with the spectrometer are in arbitrary units, as now indicated in the figure caption, and NIST data are only relative values in a limited interval (described in the referenced literature).**

P7L170–172: Move to introduction.

These publications are also referred in the introduction. We believe that this comparison to the literature is essential for the discussion here.

P7L178: Give the full name of "RIMS". 4

The full name was previously given in Line 174.

P7L183–187: Move to introduction.

changed accordingly

P8L192–193: Please keep consistency, either use % or mg/kg for mass fraction.

corrected

P10L244: If refer to organics, m/z 39+ should be C3H3+.

corrected

P10L245–252: Move the data analysis part to the method section.

changed accordingly

P11L259: Add more references for TMA, e.g., Angelino et al., 2001; Pratt et al., 2009; Köllner et al., 2017.

Köllner et al., 2017 added

P11L269–270: What it the threshold of Fe signal(s) to identify Fe-containing particles.

After resampling and baseline correction of the raw data, a peakfinder algorithm from the bioinformatics toolbox of matlab was used to identify peaks. The prominence threshold value was 1.5, which was determined in extensive tests on many individual particles by hand. Subsequently, 50% of the single spectra showing 54Fe in the algorithm (black bars in Fig. 5) were manually cross-checked. Consequently, we are very confidential that we correctly identified the Fe-containing particles with virtually no false positive results.

changes made to the manuscript:

- **We added a statement on the manual cross-check to the text.**

P12L290–292: Fe can be detected in different particle types does not suggest less particle matrix effect. Please see the first major comment and rephrase the sentence, as well as the following statement.

changes made to the manuscript:

- **As previously discussed, we rephrased this sentence according to the reviewer's comments.**
  "This suggests that the resonant ionization allows a more universal and secure detection of Fe."

Supplement Figure S4: Can you really detect particles in the size range from 0 to 200 nm? What is the detection limit of this instrument? Please add such information in the method section in the main manuscript, and only show the data within the detection limits.

Similar to other instrumental realizations using large, ellipsoidal mirrors guiding scattered light to the photomultipliers, such as ATOF-MS (Su et al., 2004) and SPLAT (Zelenyuk et al., 2005), the detection efficiency drops below about 250 nm and it approaches zero around 100 nm. The efficiencies and limits of our instrument are published in the referred literature (Li et al., 2011)

changes made to the manuscript:

- **We changed the size distribution plots according to the suggestions of the reviewer and removed the particle counts up to 200 nm size, which may result from artefacts.**

References:

Angelino, S., Suess, D. T., and Prather, K. A.: Formation of aerosol particles from reactions of secondary and tertiary alkylamines: Characterization by aerosol time-of-flight mass spectrometry, Environ Sci Technol, 35, 3130–3138, 2001.

Dall'Osto, M., Beddows, D. C. S., Harrison, R. M., and Onat, B.: Fine Iron Aerosols Are Internally Mixed with Nitrate in the Urban European Atmosphere, Environ. Sci. Technol., 50, 4212–4220, doi:10.1021/acs.est.6b01127, 2016.

Furutani, H., Jung, J., Miura, K., Takami, A., Kato, S., Kajii, Y., and Uematsu, M.: Single-particle chemical characterization and source apportionment of iron-containing atmospheric aerosols in Asian outflow, J. Geophys. Res., 116, 5504, doi:10.1029/2011JD015867, 2011.

Hatch, L. E., Pratt, K. A., Huffman, J. A., Jimenez, J. L., and Prather, K. A.: Impacts of aerosol aging on laser desorption/ ionization in single-particle mass spectrometers, Aerosol Sci. Tech., 48, 1050–1058, 2014.

Köllner, F., Schneider, J., Willis, M. D., Klimach, T., Helleis, F., Bozem, H., Kunkel, D., Hoor, P., Burkart, J., Leaitch, W. R., Aliabadi, A. A., Abbatt, J. P. D., Herber, A. B., and Borrmann, S.: Particulate trimethylamine in the summertime Canadian high Arctic lower troposphere, Atmos Chem Phys, 17, 13747–13766, 2017.

Li, L., Huang, Z., Dong, J., Li, M., Gao, W., Nian, H., Fu, Z., Zhang, G., Bi, X., Cheng, P., and Zhou, Z.: Real time bipolar time-of-flight mass spectrometer for analyzing single aerosol particles, Int. J. Mass Spectrom., 303, 118–124, doi:10.1016/j.ijms.2011.01.017, 2011.

Li, W., Xu, L., Liu, X., Zhang, J., Lin, Y., Yao, X., Gao, H., Zhang, D., Chen, J., Wang, W., Harrison, R. M., Zhang, X., Shao, L., Fu, P., Nenes, A., and Shi, Z.: Air pollution-aerosol interactions produce more bioavailable iron for ocean ecosystems, Sci. Adv., 3, e1601749, doi:10.1126/sciadv.1601749, 2017.

Moffet, R. C., Furutani, H., Rödel, T. C., Henn, T. R., Sprau, P. O., Laskin, A., Uematsu, M., and Gilles, M. K.: Iron speciation and mixing in single aerosol particles from the Asian continental outflow, J. Geophys. Res., 117, doi:10.1029/2011JD016746, 2012.

Pratt, K. A., Hatch, L. E., and Prather, K. A.: Seasonal Volatility Dependence of Ambient Particle Phase Amines, Environ Sci Technol, 43, 5276–5281, 2009.

Pratt, K. A., Mayer, J. E., Holecek, J. C., Moffet, R. C., Sanchez, R. O., Rebotier, T. P., Furutani, H., Gonin, M., Fuhrer, K., Su, Y., Guazzotti, S., and Prather, K. A.: Development and characterization of an aircraft aerosol time-of-flight mass spectrometer, Anal. Chem., 81, 1792–1800, doi:10.1021/ac801942r, 2009.

Reinard, M. S. and Johnston, M. V.: Ion formation mechanism in laser desorption ionization of individual nanoparticles, J. Am. Soc. Mass Spectrom., 19, 389–399, doi:10.1016/j.jasms.2007.11.017, 2008.

Shen, X., Ramisetty, R., Mohr, C., Huang, W., Leisner, T., and Saathoff, H.: Laser ablation aerosol particle time-of-flight mass spectrometer (LAAPTOF): Performance, reference spectra and classification of atmospheric samples. Atmos. Meas. Tech., 11, 2325–2343, 2018.

Su, Y., Sipin, M. F., Furutani, H., and Prather, K. A.: Development and characterization of an aerosol time-of flight mass spectrometer with increased detection efficiency, Analytical chemistry, 76, 712–719, doi:10.1021/ac034797z, 2004.

Vera, C. C., Trimborn, A., Hinz, K.-P., and Spengler, B.: Initial velocity distributions of ions generated by in-flight laser desorption/ionization of individual polystyrene latex microparticles as studied by the delayed ion extraction method, Rapid Commun. Mass Spectrom., 19, 133–146, doi:10.1002/rcm.1753, 2005.

Zelenyuk, A. and Imre, D.: Single Particle Laser Ablation Time-of-Flight Mass Spectrometer: An Introduction to SPLAT, Aerosol Science and Technology, 39, 554–568, doi:10.1080/027868291009242, 2005.

Zimmermann, R., Ferge, T., Gälli, M., and Karlsson, R.:Application of single-particle laser desorption/ionization time-of-flight mass spectrometry for detection of polycyclic aromatic hydrocarbons from soot particles originating from an industrial combustion process, Rapid Commun. Mass Spectrom., 17, 851–859, doi:10.1002/rcm.979, 2003.

Response to Anonymous Reviewer #2
We thank the reviewer for the valuable comments. Please see our reply below.

Note:
Reviewer comments are in italics.
Author responses are in normal format.
Changes that were made to the manuscript are in **bold** face with examples of the new text in blue.

"[…]With the acceptation of some minor improvements in the reporting of the results, the technical merits of the manuscript is good. However there are some major concerns about the atmospheric relevance of the field study presented. Whilst this field data supports the technical development, it does not offer insight into the atmospheric implications of the presence of Fe in the environment in which it was measured. As this is a key requirement of this journal, the authors are requested to provide this discussion or consider submitting to a technical journal such as AMT."

With our study, we aim on a broad scientific audience including scientists who are more focused on interactions between the atmosphere, the oceans and the biosphere than on specialized measurement technologies. To draw their attention to the application potential of our study, e.g. for existing and future interdisciplinary projects on micronutrient cycles, we aim on the publication in ACP as an open-access journal with large outreach. However, the data shown in our study already provide interesting insights into atmospheric iron transport pathways. Therefore, we extended the discussion of our data and its implications for previous as well as future studies on metal transport.
changes made to the manuscript:

- **We added a new part discussing the mixing state of Fe-containing particles, compared it to previous studies and discussed implications for future studies.**
  "Although our field study provides only a limited dataset, some general implications can already be derived. The internal mixing of Fe with sulfate or organic acids is assumed to be crucial for Fe dissolution, and thus for the anthropogenic increase of bioavailable iron input to the oceans (Li et al., 2017). Previous studies indicated that the Fe transport into the sea is dominated by coal combustion particles containing sulfate in Asia (Furutani et al., 2011; Moffet et al., 2012), while the majority of Fe-containing particles in Europe are mixed with nitrate and were attributed to traffic activities (Dall'Osto et al., 2016). Similar to our experiment, these studies found strong internal mixing of many Fe-containing particles, such as biomass burning signals with coal combustion contributions in Asia and secondary nitrate with Fe in Europe. However, Fe-particles with sea-salt signatures were negligible in the SPMS studies and mixtures of Fe and OC were a minor fraction (Furutani et al., 2011; Dall'Osto et al., 2016). In our study, these particles were the most abundant types of Fe-containing particles, if resonant ionization was applied, see Fig 5(b), while for non-resonant ionization, particles with EC signatures were dominant (Fig. 5(a)). Taking into account that the aforementioned SPMS studies utilized non-resonant LDI of Fe at 266 nm, Fe-transport in organic and salt/mixed aerosols might have been underestimated. Electron microscopy studies of individual particles in Asia frequently revealed thick coatings of secondary compounds and organic matter around Fe-rich particle components (Li et al., 2017; Moffet et al., 2012). Ultra-fine Fe-containing particles, such as soot from traffic emissions, can enter the long-range transported accumulation mode via agglomeration with larger particles and condensation of organic vapours, secondary nitrate or sulfate. In our study, we observed a high prevalence of Fe in sea salt and OC particle types, indicating the importance of these pathways for transport of biologically relevant Fe."

- **The conclusion section was extended to better address the general implications for SPMS applications in atmospheric chemistry.**
  "Not all physical details are fully understood, and the signal enhancement effects providing the basis for the improved metal detection efficiency are difficult to quantify for the different particle types. However, our results show that the increase in sensitivity is moderate for particular Fe-rich aerosols, such as the about 3-fold signal enhancement for Arizona test dust. The resonance enhancement appears to become more effective for mixed particles with smaller Fe-contributions such as in the ambient air experiment, where about 10 times more particles revealed Fe-signatures in direct comparison with non-resonant ionization. Taking into account the lower hit rate of the KrF laser, a downside related to its lower photon energy, the overall efficiency to identify Fe signatures in a single-particle mass spectrum was increased by a factor of about 20 in our ambient air study.
  The coincidental matching of the KrF laser line with a strong absorption of Fe atoms allows an easy and straightforward application of the resonance effect in the field. For direct comparison of KrF with ArF lasers, it has to be considered that the lower photon energy of KrF laser is associated with a reduced hit

rate and different mass spectral signatures of other particle components, e.g. organics. Further studies are required to evaluate these differences. Of note, because of its rather high pulse energy and the flat-top beam profile, the hit rate of the KrF laser was about 40−50 % in our experiment, which is still more than the values that are typically achieved with the most common laser line in SPMS, the Nd:YAG at 266 nm. Exploiting the resonance effect for other metals than Fe requires a tuneable Nd:YAG-OPO system, which is, however, more difficult to operate."

Minor Comments:

L51 Most of the iron in mineral dust is in the form Fe2O3 (hematite) which is also insoluble. A distinction between soluble and insoluble Fe should be made as it affects bioavailiblity which is a major justification for carrying out this work.

We rephrased the respective sentence to make the distinction clearer.

- **changes made to the manuscript:**
  "The highly soluble, and thus more bioavailable Fe from anthropogenic aerosols that adds to the larger flux of rather insoluble mineral dust…"

L59 Replace 'were' with 'have been'.
corrected

L61 Replace/remove 'herein', as it implies it is a feature if this study.
corrected

L63 Not all SPMS is bipolar, e.g. PALMS.
corrected - statement on both polarities removed

L64 Replace 'typical ionization products' with 'typical observed ions'
corrected

L65 It would be useful to be more specific about which metals have been detected. Provide some references.

- **We added a new sentence with examples and references.**
  "For example, vanadium can indicate ship emissions (Healy et al., 2009; Ault et al., 2010) and signal patterns of e.g. aluminium, silicon and calcium point on soil dust particles (Sullivan et al., 2007)."

L68 The matrix effect will influence all compounds, not just the minor ones. The description of the matrix effect should be developed further.

- **We rephrased the sentence and provided a clear link between the matrix effects and its physical origins that are provided in the following sentence.**
  "For example, the particle's humidity and its main composition can have a strong effect on the detection of particle compounds (Neubauer et al., 1998), known as matrix effects. These effects are associated with several poorly determined interactions at the particle surface and in the desorbed plume affect ion formation (Reilly et al., 2000; Reinard and Johnston, 2008; Hinz and Spengler, 2007; Murphy, 2007; Wade et al., 2008; Hatch et al., 2014; Schoolcraft et al., 2000), reduce detection efficiencies and complicate quantification approaches (Healy et al., 2013; Gemayel et al., 2017; Gross et al., 2000; Fergenson et al., 2001; Qin et al., 2006; Zhou et al., 2016; Shen et al., 2019)"
- **Furthermore, we specified our statements on matrix effects and removed this term from the discussion of our results, as suggested by reviewer 1.**

L75 The description of LDI and REMPI are a little conflated. It would be easier to follow if they were described in separate paragraphs. It should also be clear when talking about the techniques generally, or specifically to SPMS. The reference Gunzer et al (2019) is a review paper not specific to SPMS for example.

- **We rephrased the sentence to be more specific here.**
  "In such a two-step approach, thermal or laser desorption (LD) is often followed by Resonance-Enhanced Multiphoton Ionization (REMPI), a gas-phase ionization technique that is highly sensitive and selective for aromatic molecules (Gunzer et al., 2019) The LD-REMPI approach yields detailed mass spectra…"

L87 The conclusions of the present study and those of Schade et al (2019) should be clearly separated.
changes made to the manuscript:

- **We removed this sentence and added the statement on the combination of both technologies in the conclusions section.**

Experimental Section:
An introductory paragraph at the start of this section would be useful to set the scene for the experimental approached that follow. A better description of the instrument geometry should be provided. The authors reference an early technical paper for the Hexin instrument (Li et al 2011) but it is unclear what other modification have been made (if any) that could influence the instrument performance. Are any prior publication made with this instrument platform (e.g. Schade et al 2019)?

changes made to the manuscript:

- **We re-structured the Experimental section (now "Methods") and introduced sub-headings, added the requested technical information and further references.**
  example on new text on the basic instrumental design:
  "Briefly, its instrumental layout is conceptually close to the ATOF-MS (Su et al., 2004) with an aerodynamic lens inlet and an optical sizing unit that comprises of a pair of 75 mW cw-lasers at a wavelength of 532 nm, ellipsoidal mirrors and photomultipliers. The dual-polarity mass spectrometer is designed in Z-TOF geometry, as introduced by (Pratt et al., 2009). For further details, e.g. the inlet particle transmission and detection efficiency, we refer to the literature (Li et al., 2011; Zhou et al., 2016). After the laboratory experiments, we implemented delayed ion extraction (Δt=0.4 µs) using high-voltage switches (HTS31-03-GSM, Behlke GmbH, Germany) to improve the peak quality in the ambient air experiments (Vera et al., 2005; Li et al., 2018)"

Results and Discussion:
A short introductory paragraph at the start of this section would also be helpful. The subsection titles should have some equivalence e.g. 3.2 Resonance enhancement of trace metals.

changes made to the manuscript:

- **We changed the subsection headings accordingly.**

In the lab experiments, why were different OPO wavelengths used for the soot (250.0nm) and test dust (242.2nm)?

We thank the reviewer for his attention. We corrected the figure and text accordingly, that both for the soot and the dust the same wavelengths are compared. Now, in all spectra, the reference wavelength is shorter, i.e. the photon energy is higher. Thus, possible effects of a higher photon energy, e.g. photoionization thresholds, are excluded and the enhancement can be attributed to the resonance with a higher level of certainty. Only for Zn, the reference wavelength is longer, which is associated with the instrument's UV limit and explained in the text.

changes made to the manuscript:

- **new Figure 1 now shows a consistent wavelength comparison for Diesel soot and Arizona dust.**
- **statement on the exception of a higher wavelength for Zn added in the text.**
- **new data shown in Supplemental Figure S5 presents three-wavelength comparison for all Fe, Mn and Zn in NIST urban dust.**

Figure1 What is the right hand axis of panel (B)?
changes made to the manuscript:

- **we removed this artefact in the new version of Figure 1.**

L152 'remarkably width'
corrected

L182-186 Seems to be introductory material. Could this be moved to the introduction?
moved to the introduction, according to the reviewer's suggestion.

L190 The NIST reference material is described as 'well characterised'. A summary of this characterisation should be given e.g. from NIST certificate of analysis https://www-s.nist.gov/srmors/certificates/1649b.pdf
We added the direct reference to the certificate in the methods section.

L200 'prove that not only the sum signals of the metals are higher in resonant case, but also more individual particles reveal their signatures.' This sentence is unclear and should be re-written with reference to limit of detection.
We rephrased the sentence. An absolute value for a limit of detection can unfortunately not be provided, but the discussion on the enhancement's magnitude was strengthened in the discussion and the conclusion.
changes made to the manuscript:

- **sentence rephrased**
  "The histogram plots (d…f) prove that the enhancement does not only result from a minority of particles that contribute especially strong ion signals. In contrary, a higher number of individual particles reveal signatures of the respective metals, which indicates a more secure and sensitive detection."
- **magnitude of enhancement discussed, e.g.**
  " …the improved metal detection efficiency are difficult to quantify for the different particle types. However, our results indicate that the increase in sensitivity is rather moderate for particular Fe-rich aerosols, such as the about 3-fold signal enhancement for Arizona test dust. The resonance enhancement appears to become more effective for mixed particles with smaller Fe-contributions like in the ambient air experiment, where about 10 times more particles revealed Fe-signatures in direct comparison with non-resonant ionization."

L213 Data that describes this instability should be provided.

- **information provided**
  In our experiments, thermal lensing problems of the irregularly triggered OPO system reduced its pulse power and stability, resulting in a shot-to-shot variability of the pulse power up to about 30 % .

Figure 4 Caption 'The two lasers fired alternately on 1500 particle each.'
corrected

*Conclusion**:** Some quantitative estimation of the enhancement achieved should be given. The trade-off between metal enhancement and lower particle detection rates should be highlighted.*
changes made to the manuscript:

- **magnitude of enhancement discussed:**
  " …the improved metal detection efficiency are difficult to quantify for the different particle types. However, our results show that the increase in sensitivity is moderate for particular Fe-rich aerosols, such as the about 3-fold signal enhancement for Arizona test dust. The resonance enhancement appears to become more effective for mixed particles with smaller Fe-contributions such as in the ambient air experiment, where about 10 times more particles revealed Fe-signatures in direct comparison with non-resonant ionization. Taking into account the lower hit rate of the KrF laser, a downside related to its lower photon energy, the overall efficiency to identify Fe signatures in a single-particle mass spectrum was increased by a factor of about 20 in our ambient air study.

References

Ault, A. P., Gaston, C. I., Wang, Y., Dominguez, G., Thiemens, M. H., and Prather, K. A.: Characterization of the single particle mixing state of individual ship plume events measured at the Port of Los Angeles, Environ. Sci. Technol., 44, 1954–1961, doi:10.1021/es902985h, 2010.

Dall'Osto, M., Beddows, D. C. S., Harrison, R. M., and Onat, B.: Fine Iron Aerosols Are Internally Mixed with Nitrate in the Urban European Atmosphere, Environ. Sci. Technol., 50, 4212–4220, doi:10.1021/acs.est.6b01127, 2016.

Fergenson, D. P., Song, X. H., Ramadan, Z., Allen, J. O., Hughes, L. S., Cass, G. R., Hopke, P. K., and Prather, K. A.: Quantification of ATOFMS data by multivariate methods, Anal. Chem., 73, 3535–3541, doi:10.1021/ac010022j, 2001.

Furutani, H., Jung, J., Miura, K., Takami, A., Kato, S., Kajii, Y., and Uematsu, M.: Single-particle chemical characterization and source apportionment of iron-containing atmospheric aerosols in Asian outflow, J. Geophys. Res., 116, 5504, doi:10.1029/2011JD015867, 2011.

Gunzer, F., Krüger, S., and Grotemeyer, J.: Photoionization and photofragmentation in mass spectrometry with visible and UV lasers, Mass Spectrom. Rev., 38, 202–217, doi:10.1002/mas.21579, 2019.

Hatch, L. E., Pratt, K. A., Huffman, J. A., Jimenez, J. L., and Prather, K. A.: Impacts of Aerosol Aging on Laser Desorption/Ionization in Single-Particle Mass Spectrometers, Aerosol Sci. Technol., 48, 1050–1058, doi:10.1080/02786826.2014.955907, 2014.

Healy, R. M., O'Connor, I. P., Hellebust, S., Allanic, A., Sodeau, J. R., and Wenger, J. C.: Characterisation of single particles from in-port ship emissions, Atmospheric Environ., 43, 6408–6414, doi:10.1016/j.atmosenv.2009.07.039, 2009.

Healy, R. M., Sciare, J., Poulain, L., Crippa, M., Wiedensohler, A., Prévôt, A. S. H., Baltensperger, U., Sarda-Estève, R., McGuire, M. L., Jeong, C.-H., McGillicuddy, E., O&apos, Connor, I. P., Sodeau, J. R., Evans, G. J., and Wenger, J. C.: Quantitative determination of carbonaceous particle mixing state in Paris using single-particle mass spectrometer and aerosol mass spectrometer measurements, Atmos. Chem. Phys., 13, 9479–9496, doi:10.5194/acp-13-9479-2013, 2013.

Hinz, K.-P. and Spengler, B.: Instrumentation, data evaluation and quantification in on-line aerosol mass spectrometry, Journal of mass spectrometry JMS, 42, 843–860, doi:10.1002/jms.1262, 2007.

Gemayel, R., Temime-Roussel, B., Hayeck, N., Gandolfo, A., Hellebust, S., Gligorovski, S., and Wortham, H.: Development of an analytical methodology for obtaining quantitative mass concentrations from LAAP-ToF-MS measurements, Talanta, 174, 715–724, doi:10.1016/j.talanta.2017.06.050, 2017.

Gross, D. S., Gälli, M. E., Silva, P. J., and Prather, K. A.: Relative Sensitivity Factors for Alkali Metal and Ammonium Cations in Single-Particle Aerosol Time-of-Flight Mass Spectra, Anal. Chem., 72, 416–422, doi:10.1021/ac990434g, 2000.

Li, L., Huang, Z., Dong, J., Li, M., Gao, W., Nian, H., Fu, Z., Zhang, G., Bi, X., Cheng, P., and Zhou, Z.: Real time bipolar time-of-flight mass spectrometer for analyzing single aerosol particles, Int. J. Mass Spectrom., 303, 118–124, doi:10.1016/j.ijms.2011.01.017, 2011.

Li, W., Xu, L., Liu, X., Zhang, J., Lin, Y., Yao, X., Gao, H., Zhang, D., Chen, J., Wang, W., Harrison, R. M., Zhang, X., Shao, L., Fu, P., Nenes, A., and Shi, Z.: Air pollution-aerosol interactions produce more bioavailable iron for ocean ecosystems, Sci. Adv., 3, e1601749, doi:10.1126/sciadv.1601749, 2017.

Moffet, R. C., Furutani, H., Rödel, T. C., Henn, T. R., Sprau, P. O., Laskin, A., Uematsu, M., and Gilles, M. K.: Iron speciation and mixing in single aerosol particles from the Asian continental outflow, J. Geophys. Res., 117, doi:10.1029/2011JD016746, 2012.

Murphy, D. M.: The design of single particle laser mass spectrometers, Mass Spectrom. Rev., 26, 150–165, doi:10.1002/mas.20113, 2007.

Neubauer, K. R., Johnston, M. V., and Wexler, A. S.: Humidity effects on the mass spectra of single aerosol particles, Atmospheric Environ., 32, 2521–2529, doi:10.1016/S1352-2310(98)00005-3, 1998.

Qin, X., Bhave, P. V., and Prather, K. A.: Comparison of two methods for obtaining quantitative mass concentrations from aerosol time-of-flight mass spectrometry measurements, Anal. Chem., 78, 6169–6178, doi:10.1021/ac060395q, 2006.

Pratt, K. A., Mayer, J. E., Holecek, J. C., Moffet, R. C., Sanchez, R. O., Rebotier, T. P., Furutani, H., Gonin, M., Fuhrer, K., Su, Y., Guazzotti, S., and Prather, K. A.: Development and characterization of an aircraft aerosol time-of-flight mass spectrometer, Anal. Chem., 81, 1792–1800, doi:10.1021/ac801942r, 2009.

Reilly, P. T. A., Lazar, A. C., Gieray, R. A., Whitten, W. B., and Ramsey, J. M.: The Elucidation of Charge-Transfer-Induced Matrix Effects in Environmental Aerosols Via Real-Time Aerosol Mass Spectral Analysis of Individual Airborne Particles, Aerosol Sci. Technol., 33, 135–152, doi:10.1080/027868200410895, 2000.

Reinard, M. S. and Johnston, M. V.: Ion formation mechanism in laser desorption ionization of individual nanoparticles, J. Am. Soc. Mass Spectrom., 19, 389–399, doi:10.1016/j.jasms.2007.11.017, 2008.

Schade, J., Passig, J., Irsig, R., Ehlert, S., Sklorz, M., Adam, T., Li, C., Rudich, Y., and Zimmermann, R.: Spatially Shaped 475 Laser Pulses for the Simultaneous Detection of Polycyclic Aromatic Hydrocarbons as well as Positive and Negative Inorganic Ions in Single Particle Mass Spectrometry, Anal. Chem., 91, 10282–10288, doi:10.1021/acs.analchem.9b02477, 2019.

Schoolcraft, T. A., Constable, G. S., Zhigilei, L. V., and Garrison, B. J.: Molecular dynamics simulation of the laser disintegration of aerosol particles, Anal. Chem., 72, 5143–5150, doi:10.1021/ac0007635, 2000.

Sullivan, R. C., Guazzotti, S. A., Sodeman, D. A., and Prather, K. A.: Direct observations of the atmospheric processing of Asian mineral dust, Atmos. Chem. Phys., 7, 1213–1236, doi:10.5194/acp-7-1213-2007, 2007

Su, Y., Sipin, M. F., Furutani, H., and Prather, K. A.: Development and characterization of an aerosol time-of flight mass spectrometer with increased detection efficiency, Analytical chemistry, 76, 712–719, doi:10.1021/ac034797z, 2004.

Shen, X., Saathoff, H., Huang, W., Mohr, C., Ramisetty, R., and Leisner, T.: Understanding atmospheric aerosol particles with improved particle identification and quantification by single-particle mass spectrometry, Atmos. Meas. Tech., 12, 2219–2240, doi:10.5194/amt-12-2219-2019, 2019.

Vera, C. C., Trimborn, A., Hinz, K.-P., and Spengler, B.: Initial velocity distributions of ions generated by in-flight laser desorption/ionization of individual polystyrene latex microparticles as studied by the delayed ion extraction method, Rapid Commun. Mass Spectrom., 19, 133–146, doi:10.1002/rcm.1753, 2005.

Wade, E. E., Farquar, G. R., Steele, P. T., McJimpsey, E. L., Lebrilla, C. B., and Fergenson, D. P.: Wavelength and size dependence in single particle laser aerosol mass spectra, J. Aerosol Sci., 39, 657–666, doi:10.1016/j.jaerosci.2008.03.007, 2008.

Zhou, Y., Huang, X. H., Griffith, S. M., Li, M., Li, L., Zhou, Z., Wu, C., Meng, J., Chan, C. K., Louie, P. K.K., and Yu, J. Z.: A field measurement based scaling approach for quantification of major ions, organic carbon, and elemental carbon using a single particle aerosol mass spectrometer, Atmospheric Environ., 143, 300–312, doi:10.1016/j.atmosenv.2016.08.054, 2016.

Resonance-Enhanced Detection of Metals in Aerosols using Single Particle Mass Spectrometry

Johannes Passig[1,2,3], Julian Schade[2,3], Ellen Iva Rosewig[2,3], Robert Irsig[3,4], Thomas Kröger-Badge[2,3], Hendryk Czech[1,2,3], Martin Sklorz[1], Thorsten Streibel[1,2], Lei Li[5], Xue Li[5], Zhen Zhou[5], Henrik Fallgren[6], Jana Moldanova[6], and Ralf Zimmermann[1,2,3]

[1]Joint Mass Spectrometry Centre, Cooperation Group 'Comprehensive Molecular Analytics' (CMA), Helmholtz Zentrum München, 85764 Neuherberg, Germany
[2]Joint Mass Spectrometry Centre, Chair of Analytical Chemistry, University Rostock, 18059 Rostock, Germany
[3]Department Life, Light & Matter, University of Rostock, 18051 Rostock, Germany
[4]Photonion GmbH, 19061 Schwerin, Germany
[5]Institute of Mass Spectrometry and Atmospheric Environment, Jinan University, Guangzhou 510632, China and Guangzhou Hexin Instrument Co., LTD, Guangzhou 510530, China
[6]IVL Swedish Environmental Research Institute, 411 33 Gothenburg, Sweden

Correspondence to: Johannes Passig (johannes.passig@uni-rostock.de)

Abstract. We describe resonance effects in laser desorption/ionization (LDI) of particles that substantially increase the sensitivity and selectivity to metals in single particle mass spectrometry (SPMS). Within the proposed scenario, resonant light absorption by ablated metal atoms increases their ionization rate within a single laser pulse. By choosing the appropriate laser wavelength, the key micronutrients Fe, Zn and Mn can be detected on individual aerosol particles with considerably improved efficiency. These ionization enhancements for metals apply to natural dust and anthropogenic aerosols, both important sources of bioavailable metals to marine environments. Transferring the results into applications, we show that the spectrum of our KrF-excimer laser is in resonance with a major absorption line of iron atoms. To estimate the impact of resonant LDI on the metal detection efficiency in SPMS applications, we performed a field experiment on ambient air with two alternately firing excimer lasers of different wavelengths. Herein, resonant LDI with the KrF-excimer laser (248.3 nm) revealed iron~~Fe~~ signatures for many more ~~aerosol~~ particles of the same aerosol ensemble compared to the more common ArF-excimer laser line of 193.3 nm (non-resonant LDI of iron). Many of the particles that showed iron contents upon resonant LDI were mixtures of sea salt and organic carbon. For non-resonant ionization, iron was exclusively detected in particles with a soot contribution. This suggests that resonant LDI allows a more universal and secure metal detection in SPMS. Moreover, our field study indicates relevant atmospheric iron transport by mixed organic particles, a pathway that might be underestimated in SPMS measurements based on non-resonant LDI. ~~Moreover, resonant ionization of iron appeared to be less dependent on the particle matrix than conventional non-resonant LDI, allowing a more universal and secure detection of Fe.~~ Our findings show a way to improve the detection and source attribution capabilities of SPMS for particle-bound metals, a health-relevant aerosol component and an important source of micronutrients to the surface oceans affecting marine primary productivity.

1 Introduction

Natural and anthropogenic aerosols play a pivotal role in global climate and biogeochemical cycles, yet limited ambient observations result in large uncertainties. While sulfate and carbonaceous aerosols are intensively investigated for their climate effects (Wang et al., 2016; Seinfeld and Pandis, 2016; Kanakidou et al., 2005; Bond et al., 2013; Sofiev et al., 2018), the particle-bound metals have far-reaching impacts on ecosystems and human health. The redox cycling activity of inhaled transition metals such as iron (Fe) induces oxidative stress and is involved in severe health effects from air pollution (Ye et al., 2018; Oakes et al., 2012; Fang et al., 2017). Furthermore, atmospheric particles are important sources of marine micronutrients (Mahowald et al., 2018; Jickells et al., 2005). The highly soluble, and thus more bioavailable Fe from anthropogenic aerosols that adds to the larger flux of rather insoluble mineral dust is assumed to affect primary production and carbon export in a significant part of the world's oceans (Ito and Shi, 2016; Li et al., 2017; Ito, 2015). Beyond Fe, further biologically important trace metals exert health effects (Gaur and Agnihotri, 2019) or can modulate primary production (Mahowald et al., 2018). For example, as enzyme co-factors they can determine which enzymes cells can express, affecting the composition of microbial communities (Boyd et al., 2017). Productivity-limiting deficiencies of e.g. manganese (Mn) and zinc (Zn) have been reported for marine regions (Mahowald et al., 2018). Zinc is also associated with toxicological responses to wood combustion aerosols (Uski et al., 2015; Kanashova et al., 2018). However, the magnitude and variability of ~~this~~ anthropogenic sources of bioavailable metals in the sea are poorly characterized. Recently, anthropogenic fluxes and sources of Fe were estimated using isotope fingerprinting (Conway et al., 2019). Such studies require measurable differences between natural and anthropogenic isotope distributions of the respective metals. Alternative methods, preferably providing detailed source information, indicating the metal's bioavailability and acquiring episodic deposition events are required to refine the global distribution models with observational data.

Several mass spectrometry based analytical techniques for aerosol characterization ~~were~~ have been developed, with single particle mass spectrometry (SPMS) being a real-time method obtaining the size and a chemical profile from individual particles (Pratt and Prather, 2012; Laskin et al., 2018). ~~Herein~~ In SPMS, the particles are introduced into a vacuum, individually sized and exposed to intense UV laser pulses that form a partly ionized plume (laser desorption/ionization, LDI) (Hinz and Spengler, 2007; Murphy, 2007). ~~Both positive and negative I~~ions are extracted and analyzed with respect to their mass-to-charge ratio (m/z). Typically ~~ionization products~~observed ions are e.g. organic fragments, salts, ammonia, nitrate, sulfate, alkali metals, mineral components such as silicate and carbon clusters from elemental or organic carbon (EC~~,~~ or OC). ~~Beyond~~Along with the single-particle aspect, SPMS stands out for its metal detection capabilities that yield unique source information data (Dall'Osto et al., 2016b; Pratt and Prather, 2012; Arndt et al., 2017; Dall'Osto et al., 2016a). For example, vanadium can indicate ship emissions (Healy et al., 2009; Ault et al., 2010) and signal patterns of e.g. aluminium, silicon and calcium point on soil dust particles (Sullivan et al., 2007). However, compound-specific ionization efficiencies differ significantly. For example, the particle's humidity and its main ~~components~~ composition can have a strong effect on the detection of ~~minor~~ particle compounds (Neubauer et al., 1998), known as matrix effects. These effects are associated with

sSeveral poorly determined interactions at the particle surface and in the desorbed plume affect ion formation (Reilly et al., 2000; Reinard and Johnston, 2008; Hinz and Spengler, 2007; Murphy, 2007; Wade et al., 2008; Hatch et al., 2014; Schoolcraft et al., 2000), reduce detection efficiencies and complicate quantification approaches (Healy et al., 2013; Gemayel et al., 2017; Gross et al., 2000; Fergenson et al., 2001; Qin et al., 2006; Zhou et al., 2016; Shen et al., 2019). These difficulties can be mitigated if the desorption and ionization are separated in a two-step process, and ions are formed by resonant ionization in the gaseous plume, as as demonstrated for aromatic hydrocarbons (Morrical et al., 1998; Bente et al., 2008; Woods et al., 2001). HereinIn such a two-step approach, thermal or laser desorption (LD) is often followed by Resonance-Enhanced Multiphoton Ionization (REMPI), a gas-phase ionization technique that is highly sensitive and selective forof the aromatic molecules (Gunzer et al., 2019). The LD-REMPI approach yields detailed mass spectra of the health-relevant polycyclic aromatic hydrocarbons (PAHs) - ubiquitous trace compounds of combustion particles (Bente et al., 2009; Li et al., 2019; Passig et al., 2017; Schade et al., 2019). Resonant laser ablation of metals, where the leading edge of the laser pulse ablates atoms from a solid sample that are then ionized by the same pulse, have been studied some time ago for Laser Microprobe Mass Analysis (LAMMA) from surfaces (Verdun et al., 1987; McLean et al., 1990). However, to our best knowledge, such effects have so far not been recognized and applied in aerosol/single particle mass spectrometry. In the current study, we report on such wavelength-dependent enhancements in LDI ion yields of transition metals from aerosol particles. Using an optical parametric oscillator (OPO), we demonstrate that besides Fe, also the sparsely detected and biologically relevant trace metals Zn and Mn can be observed in anthropogenic particles with much higher sensitivity. We show that the resonant absorption of iron coincides with the spectrum of the field-deployable KrF-excimer laser and with the REMPI absorption spectra of most aromatic molecules. Thus, the enhanced detection sensitivity for metals can be combined with detailed spectra of aromatic substances via REMPI. (Schade et al., 2019). This is of importance for health-related studies, as two of the most relevant adverse aerosol compounds, transition metals and PAHs, can be addressed with the same, easily accessible excimer laser wavelength. Finally, we demonstrate the application potential of the resonance effects in a field study comparing the KrF-excimer laser with a commonly used ArF-excimer laser for their Fe detection capabilities in ambient aerosols. We found that resonant LDI also reveals Fe-signatures in particle types that produced no Fe-signals upon non-resonant LDI, suggesting that the relevance of organic aerosols and salts as source for Fe might have been underestimated in earlier SPMS studies.

2 Experimental SectionMethods

2.1 Single-particle mass spectrometer and optical setup

The basic SPMS-instrument (Hexin Instruments Ltd., Guangzhou, P.R. China and Photonion GmbH, Schwerin, Germany) is described in other publications (Li et al., 2011). Briefly, its instrumental layout is conceptually close to the ATOF-MS (Su et al., 2004) with an aerodynamic lens inlet and an optical sizing unit that comprises of a pair of 75 mW cw-lasers at a wavelength of 532 nm, ellipsoidal mirrors and photomultipliers. The dual-polarity mass spectrometer is designed in Z-TOF geometry, as introduced by (Pratt et al., 2009). For further details, e.g. the inlet particle transmission and detection

efficiency, we refer to the literature (Li et al., 2011; Zhou et al., 2016). After the laboratory experiments, we implemented delayed ion extraction (Δt=0.4 µs) using high-voltage switches (HTS31-03-GSM, Behlke GmbH, Germany) to improve the peak quality in the ambient air experiments (Vera et al., 2005; Li et al., 2018). Major modifications to the commercial device comprise the ionization laser and the optical setup. We equipped the instrument~~it~~ with both a tuneable laser system (optical parametric oscillator, OPO) and excimer lasers (λ=248 nm and λ=193 nm) and replaced the Nd:YAG solid-state laser (λ=266 nm, 4^{th} harmonic frequency) that belongs to the instruments standard configuration. Apart from the wavelength, most beam parameters were comparable throughout the experiments, see Table 1 for details. The pulse energy was measured at the optical entrance and exit of the mass spectrometer and the position of the focal lens (f=200 mm) was adjusted to maintain a comparable spot area, respective intensity for all wavelength comparison experiments. The OPO wavelengths as well as the KrF-excimer laser spectrum were measured with a LRL-005 spectrometer (MK Photonics Inc. U.S.).

2.2 Data analysis

In the laboratory experiments, only particles with both a ~~meaningful~~ positive and negative ion spectrum, each showing at least two peaks above the noise level, were considered. Raw time-of-flight data was converted to mass spectra considering peak area within nominal mass resolution by custom software on Matlab platform (MathWorks Inc.). For particle classification in the ambient air study, w~~W~~e utilized the adaptive resonance theory neural network, ART-2a (Song et al., 1999) from the open-source toolkit FATES (Flexible Analysis Toolkit for the Exploration of SPMS data) (Sultana et al., 2017). w~~W~~ith a learning rate 0.05, a vigilance factor of 0.8 and 20 iterations.

2.3 Model particles, sampling and setup for ambient air experiments

Diesel exhaust particles from an old van (Volkswagen Transporter 1.7 D, build 1988) were collected from the inner surface of the exhaust tube. These particles exhibit a rather uniform chemical composition as demonstrated in previous experiments (Passig et al., 2017; Schade et al., 2019). Model particles for mineral dust were Arizona test dust 0-3 µm diameter (Powder Technology Inc., U.S.) and complex anthropogenic aerosols with trace metals were ~~modelled~~mimicked using NIST urban dust 1649b (Gonzalez and Choquette, 2016). Using a turntable-based powder disperser (Model 3433, TSI Inc., U.S.), particles were introduced into a 1 l/min carrier gas stream (N_2, purity: 5.0) from which 0.1 l/min were guided in an isokinetic flow into the instrument. For the experiments on ambient air, the SPMS instrument was set up at a meteorological station in a rural environment at the Swedish west coast, about 30 km south of Gothenburg (coordinates 57°23'37.8"N, 11°54'51.4"E). Ambient air was sampled at a height of 7 m above ground (15 m above sea level). Aerosols from a 300 l/min intake airflow were concentrated into the 1 l/min carrier gas stream using a first virtual impactor device (Model 4240, MSP corp., U.S.). After passing a dryer (Model MD-700-12S-1, Perma Pure LLC, U.S.), they were further concentrated to 0.1 l/min in a second step directly at the SPMS aerodynamic lens inlet. The concentration is most effective for particles around 1 µm size, while it drops below 0.5 µm, see Supplemental Fig. S1 for a comparison of particle numbers in ambient air with and without using the concentrator. The two KrF and ArF excimer lasers used in this experiment were alternately triggered to particles

using a custom electronic circuit based on a complex programmable logic device (Intel Max V) with 8.5 ns pin-to-pin delay and programmed using Very High Speed Integrated Circuit Hardware Description Language (VHDL). The excimer laser beams~~and their beams~~ were focused from opposite sides onto the particle beam, see Table 1 and section 3.3 for details.

Table 1. Light sources and details of the optical setup.

Laser source	Opolette HE 355 LD UV, Opotek LLC, U.S.	PhotonEx, Photonion GmbH, Germany	ATLEX-I 300, ATL GmbH, Germany
Laser medium	Optical Parametric Oscillator, Nd:YAG pumped	KrF gas (excimer)	ArF gas (excimer)
Wavelength (nm), photon energy (eV)	tuneable 210–~~...~~2400	248, 4.99	193, 6.41
Pulse duration (ns)	≈5		
Beam size (mm)	Ø3 nearly Gaussian	3x6 Gaussian x flat top	3x6 Gaussian x flat top
Interaction spot distance to focus (mm)	≈8–~~...~~11	7	7
Rayleigh length (mm)	≈1.2–~~...~~1.5	1.4	1.1
Interaction spot size (µm)	Ø160	105×~~x~~210	105×~~x~~210
Pulse energy (mJ)	0.4	3	
Pulse intensity at interaction spot (GW/cm^2)	0.8	5	

3 Results and discussion

3.1 Resonance enhancements of Fe signals

We measured the Fe signals from diesel soot and Arizona desert dust particles as representative models of relevant anthropogenic and natural aerosols transporting Fe into the oceans. Figure 1 (a) and (b) show the respective mass spectra of positive and negative ions from LDI with two different wavelengths using the OPO. The mass spectra were accumulated over each 400 particles, without normalization or further processing. The observed peak broadening results mainly from ~~averaging~~ accumulation over single particle spectra with varying ion energy and starting positions. Typical signatures for (diesel) engine emissions (Toner et al., 2006) are recognizable, e.g. clusters of elemental carbon (EC, from soot) and organic hydrocarbon fragments (OC) (Silva and Prather, 2000). Also, alkali metals are frequently detected due to their low ionization energy. The desert dust particles (Fig. 1b)) reveal typical mineral dust signals from metals and metal oxides (Sullivan et al., 2007; Dall'Osto et al., 2010). The slightly different laser wavelengths yield rather similar mass spectra~~, apart from some fragmentation differences for the soot particles in Fig. 1(a).~~. However, much stronger Fe-signals can be observed for 248.3 nm for both particle types (see insets in Fig. 1(a) and (b)). This wavelength matches the $3d^64s^2 \rightarrow 3d^64s4p$ transition of Fe atoms, a line that is also typically used for Fe determination in atomic absorption spectroscopy. As apparent from the

histogram plots in Figure 1 (c) and (d), the enhancement effect is not resulting from some especial Fe-rich particles. Instead, most particles show higher Fe-signals at the resonance wavelength and the fraction of particles without Fe-signals drops considerably. However, the high Fe-content of Arizona dust particles (≈4-7%) often leads to saturated signals on the single-particle level. Even stronger saturation effects producing highly corrupted Fe-peaks were observed for hematite, which is consequently not shown here. ~~and interferences with~~ Because interferences with CaO^+ and organic fragments such as $C_3H_4O^+$ can ~~reduce~~ affect the signal differences at m/z=56. ~~Therefore,~~ the histograms show the signal of the ^{54}Fe isotope. Contributions from organic fragments to m/z=54 are assumed to be rather small, as apparent from the signal strengths of principal fragments in the respective mass range at m/z=51, 53 and 55, see inset of Figure 1(a). However, such interferences might lead to a moderate underestimation of the resonance enhancement. A further resonance ~~enhancement~~ effect can be noticed for Lithium at the reference wavelength of 242.2 nm because of the $1s^22s \rightarrow 1s^27p$ transition close~~d~~ to this wavelength. Experimental results on hemoglobin powder, representing a particle model with uniform organic composition, are shown in Supplemental Fig. S4 and confirm the resonance enhancements for Fe.

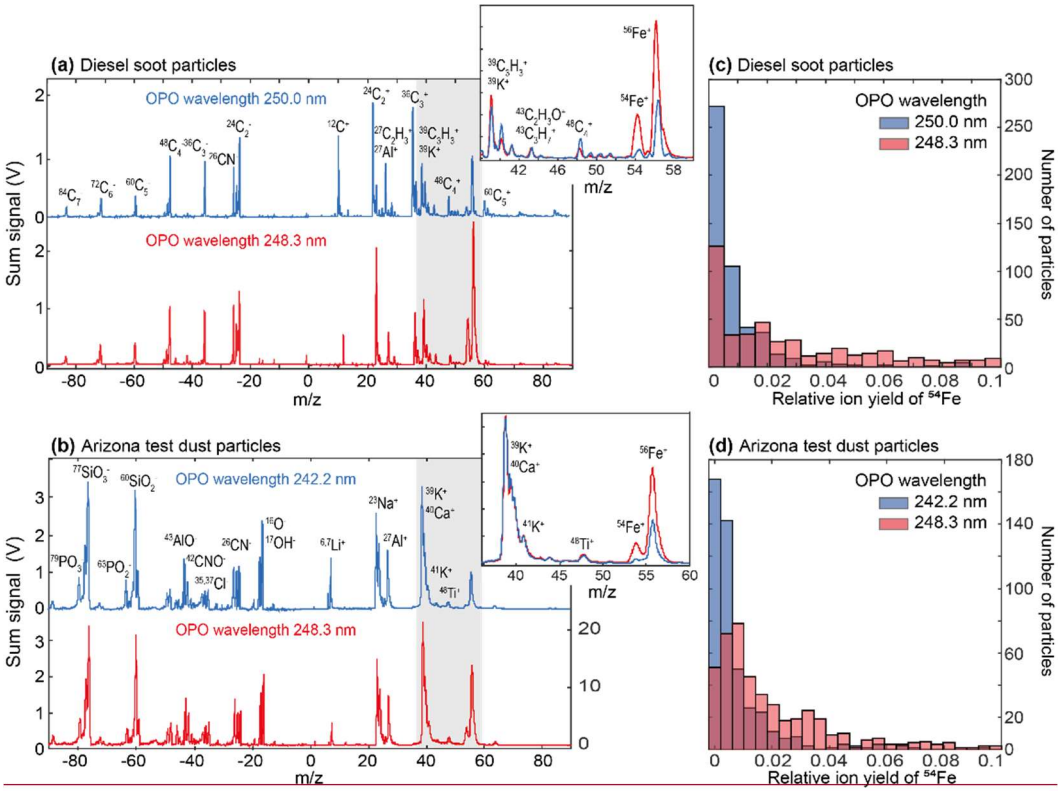

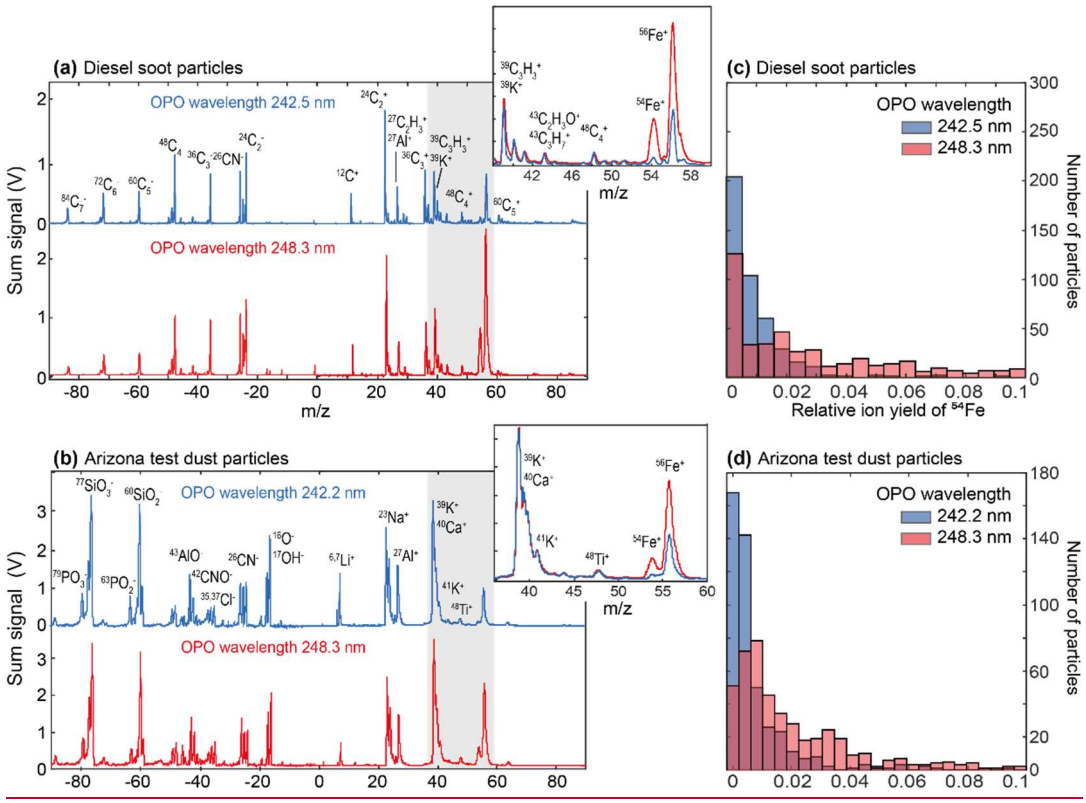

Figure 1: (a) Accumulated mass spectra (each n=400) of re-dispersed diesel soot particles ionized using the tuneable OPO laser. In the case of resonant ionization of Fe at 248.3 nm (red), the Fe signal is substantially enhanced compared to the non-resonant ionization at ~~250.0~~242.5 nm (blue), see the inset for an enlarged view of the grey area. Most other signals are similar. (b) A comparable Fe-enhancement can be observed for mineral dust particles. The histogram plots (c) and (d) of the single-particle relative ion signal ($^{54}Fe^+$ signal normalized to the particle's total ion yield) illustrate that the ionization enhancement accounts for the majority of analyzed particles. Corresponding~~The~~ normalized mass spectra are shown in Supplemental Fig. S2 and the particle size distributions are depicted~~shown~~ in Supplemental Fig. S~~3~~4.

To further investigate the enhancement effects, we measured the wavelength-dependent total ion yield of ^{54}Fe from each 12400 particles, exposed to OPO laser pulses of the same intensity. As shown in Figure 2, the maximum Fe-signal is achieved near the resonance, with an enhancement of about 3-4 for diesel soot and mineral dust particles as well as for hemoglobin particles, see Supplemental Fig. S4. The ion yield curves have a remarkably width ~~remarkably width~~ and are much broader than the atomic lines or the OPO-linewidth (4…6 cm^{-1}). The absorption spectrum of Fe-atoms (blue) represents data from the NIST atomic spectra library (Kramida and Ralchenko). Such signal enhancements at specific wavelengths were not reported in previous SPMS studies, apart from the aforementioned REMPI-techniques. Thomson et al. (1997) observed for different salts, that the threshold intensity for ion formation decreased with increasing absorbance of the bulk material~~material~~ (Thomson et al., 1997). Generally, more substances are ionized at higher photon energies and lower laser intensities are required, but these effects tend to saturate at higher laser intensities (Thomson et al., 1997; Murphy,

2007). Even in a study using two matrix-assisted LDI (MALDI) matrix materials absorbing at different wavelengths, Wade et al. (2008) found only minimal~~um~~ wavelength effects on ion yields but a stronger dependence on the intensity and particle size. (Wade et al., 2008). ~~–~~However, these results are not conflicting with the Fe resonance we observed. Several studies indicate that above a minimum intensity, effects in the plume dominate the ionization yield rather than the absorbance of the particle itself (Carson et al., 1997; Wade et al., 2008; Reinard and Johnston, 2008). The resonance begins to take effect as soon as Fe atoms are formed and vaporized from the particle during the initial phase of the laser pulse.

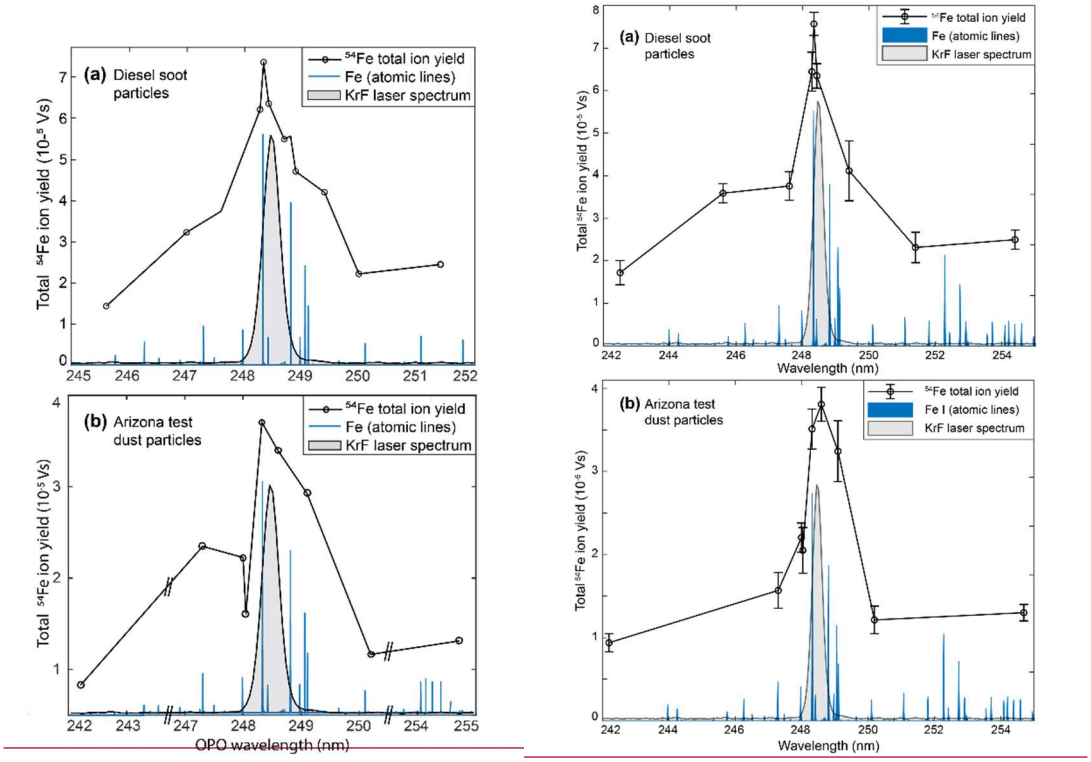

Figure 2: Wavelength-dependent total ion yield of ^{54}Fe in SPMS of re-dispersed particles (black circles, ~~each n=400~~n=1200, three replicates of 400 each). Both for (a) diesel soot particles and (b) Arizona desert dust particles, the signal peaks for wavelengths that match a major atomic transition of Fe (blue lines). The large width of the curve is attributed to line broadening through interaction with the dense particle surface. Coincidentally, the Fe-lines are also addressed by our KrF-excimer laser (measured spectrum in grey, arbitrary units). Atomic spectra from the NIST library (Kramida and Ralchenko). Mass spectra are shown in Figure 1, the respective curves of the normalized ion signals and size distributions in Supplemental Fig. S3. ~~and size distributions in Supplemental Fig. S4.~~

While so-far not recognized for SPMS, such resonance enhancements were previously reported and explained for laser ablation from solid surfaces. Using dye lasers, about five-fold signal increases were observed at the atomic lines of several metals and semiconductors (Verdun et al., 1987). The widths of the resonances were also rather broad, 0.4-0.7 nm. For low laser intensities, grazing incidence and two-step excitation, the width dropped below 0.05 nm (McLean et al., 1990) approaching the values of the respective atoms in gas phase ionization (Resonant Ionization MS, RIMS (Young et al., 1989)). The explanation for the broad signals in resonant ablation from surfaces and particles is rather simple: Broadening and transition wavelength shifts can be expected if the excitation happens when atoms are still bound in the matrix close to

the surface (Verdun et al., 1987; McLean et al., 1990). Also the plasma pressure could contribute to these effects. With increasing time and distance from the dense target, the surface bonds vanish and the conditions become similar to RIMS. Minor contributions to the measured width could result from Stark broadening (typically at higher laser power (Hübert and Ankerhold, 2011)) and from interferences with the adjacent absorption lines.

3.2 Resonant~~t Ionization~~ce enhancements of ~~T~~trace m~~M~~etals

~~Beyond Fe, further biologically important trace metals exert health effects~~ (Gaur and Agnihotri, 2019)~~ or can modulate primary production~~ (Mahowald et al., 2018)~~. For example, as enzyme co-factors they can determine which enzymes cells can express, affecting the composition of microbial communities~~ (Boyd et al., 2017)~~. Productivity-limiting deficiencies of e.g. manganese (Mn) and zinc (Zn) have been reported for marine regions~~ (Mahowald et al., 2018)~~. Zinc is also associated with toxicological responses to wood combustion aerosols~~ (Uski et al., 2015; Kanashova et al., 2018)~~.~~The resonant ionization of particle-bound Fe raises the question whether the SPMS-based detection of other biologically relevant ~~these~~ metals may also benefit from the enhancement. We used NIST Reference Material Urban Dust 1649b (National Standard Institute of Technology – U.S.) as a well-characterized anthropogenic particle model containing several transition metals at low concentrations. Figure 3 shows accumulated cation mass spectra from resonant and non-resonant ionization with respect to strong atomic lines of Fe, Mn and Zn. The mass fraction of Fe is rather high (≈3%) and the signal enhancement at 248.3 nm (see Fig. 3(a)) corresponds to the results from diesel soot and Arizona dust. Manganese contributes a mass fraction of only ~~240~~ 0.024 % ~~mg/kg~~ to the dust. In general, for particles with organic content, the Mn signature at m/z=55 can hardly be distinguished from molecular fragments of the same mass. However, when the OPO wavelength is in resonance with the $3d^5 4s^2 \rightarrow 3d^5 4s4p$ transition of Mn at 279.5 nm, a clear signal appears at m/z=55, nearly as high as the peak of the much more abundant ^{56}Fe in the sum spectrum, see Fig. 3(b). Also for Zn (mass fraction 0.17%), there is a substantial difference and a clear signature appears in resonance case (Fig. 3(c)). Because the resonance wavelength of 213.8 nm is near the UV-limit of the OPO, the pulse energy of 0.25 mJ is lower than for the other metals and, in contrary to all other wavelength comparisons, the reference wavelength is higher than the resonance wavelength. After resonant excitation at the respective wavelength, the absorption of a further single photon is sufficient for ionization of all three metals. The histogram plots (d…f) prove that the enhancement does not only result from a minority of particles that contribute especially strong ion signals. ~~not only the sum signals of the metals are higher in resonant case, but also~~ In contrary, ~~more~~ a higher number of individual particles reveal ~~their~~ signatures of the respective metals, which indicates a more secure and sensitive detection. The results suggest that tuneable laser systems can be advantageous to enhance the detectability of various elements of interest in SPMS.

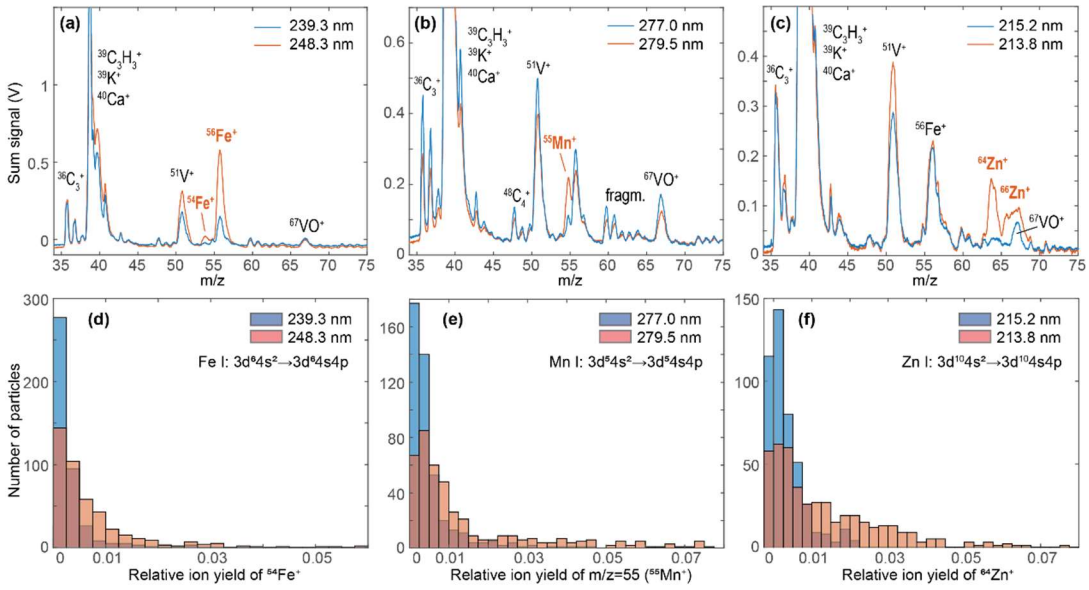

Figure 3: Accumulated cation mass spectra (n=400) of re-dispersed urban dust particles (Reference Material NIST 1649b). Using the tuneable OPO, the spectra were recorded at resonance wavelengths of each metal (red) and for the non-resonant case at a slightly different wavelength (blue). While carbon and molecular fragment signals are similar in the pairwise comparison, the resonant enhancements for (a) Fe, (b) Mn and (c) Zn are clearly visible. Complete, bipolar mass spectra and the size distribution are shown in Supplemental Fig. S5~~1~~. ~~and S4, respectively.~~ (d-f) The single-particle distribution of the relative ion signals illustrates that the resonant ionization enhancement allows metal detection for many more particles. The respective resonance wavelengths (red) address the indicated transitions.

3.3 Application to long-range transported aerosols

While our laboratory experiments revealed remarkable resonance effects for several metals and particle types, these results have to be transferred into application on ambient aerosols. Tuneable laser systems are of limited suitability for field studies because of their complexity, low pulse power and repetition rate. In our experiments, thermal lensing problems of the irregularly triggered OPO system reduced its pulse power and stability, resulting in a shot-to-shot variability of the pulse power up to about 30 %. However, a freely triggerable OPO-SPMS with sufficient pulse energy is under development. In contrast to tuneable light sources, excimer lasers are cheaper, more robust and powerful. Of note, the KrF-excimer laser line at 248.3 nm coincidentally matches the strongest UV absorption line of Fe, a fact that gained little attention in the last decades (Trainor and Mani, 1978; Seder et al., 1986). The spectrum of our laser is shown in Fig. 2. We directly compare the Fe detection efficiencies of two field-deployable excimer lasers for the same ambient aerosol ensemble. The KrF-line is in resonance with the Fe absorption, while the often-used ArF-line is not. To exclude all effects from different instrumentation, both lasers are integrated into the same SPMS, firing with the same pulse parameters from opposite sites onto the particles, see Figure 4(a) and Table 1. A custom electronic circuit triggers the lasers alternately. With regard to the important application of detecting Fe-containing aerosols in remote regions, we designed our experiment to observe long-range transported anthropogenic particles with high secondary contributions in a marine environment. Therefore, we set up our

instrument at the Swedish west coast and measured aerosols from central Europe after transport over the Baltic Sea, see the back-trajectories in Fig. 4(b).

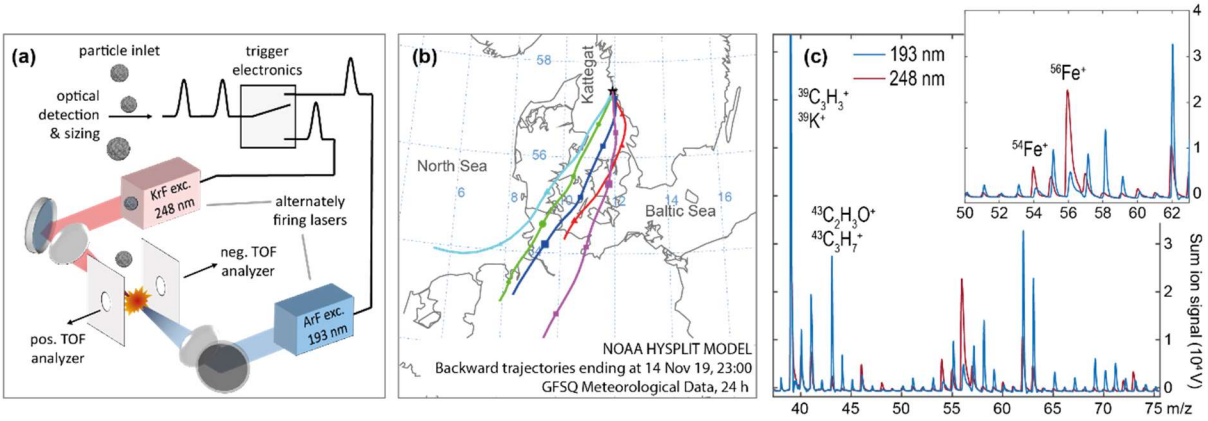

Figure 4: (a) Schematic view of the setup for direct comparison of non-resonant and resonant ionization of Fe in ambient air particles using the same mass spectrometer. The two lasers fired alternately on ~~each~~ 15,000 particles each. (b) Back-trajectories from the HYSPLIT webtool (www.ready.noaa.gov/HYSPLIT.php), ending at the sampling site (sea level) during the experiment on long-range transported particles. (c) Accumulated cation mass spectra (each n=15,000) show a Fe^+-signal enhancement for ionization with the KrF excimer laser (248 nm, red) versus the ArF excimer laser (193 nm, blue). Further differences will be discussed in a different publication.

With each of the lasers, we analyzed 15,000 individual particles on the 14 November 2019 between 15:00 and 24:00 local time. The mean particle mass concentration was 7.8 µg/m^3 (PM2.5) and 5.0 µg/m^3 (PM1.0) as measured by the station's dust monitor (Grimm EDM-180 MC). Figure 4(c) shows the resulting sum mass spectra of cations for each ionization wavelength. ~~The improved peak quality compared to Figs. 1 and 3 was achieved by implementing delayed ion extraction~~ (Vera et al., 2005; Li et al., 2018). ~~=~~The enhanced Fe signature for the KrF-laser is clearly visible in the sum spectrum. All further wavelength-dependent differences will be discussed in a future publication. From each 15,000 particles exposed to the ArF-laser (KrF-laser), 13,776 (6,364) produced a negative spectrum, 12,217 (5,577) a positive signature and 12,189 (5,258) yielded bipolar mass spectra. The higher hit rate of the ArF laser results from the lower intensity thresholds for ion formation due to its higher photon energy (Thomson et al., 1997), thus yielding mass spectra also from particles that were not fully hit. Nearly all particles (>98 %) with negative spectra showed nitrate ($^{46}NO_2^-$ and $^{62}NO_3^-$). Because the steady onshore wind during the experiment excludes local sources of nitrate, these ions indicate condensation of NO_3 and replacement of Cl^- by NO_3^- (Gard et al., 1998; Arndt et al., 2017; Dall'Osto et al., 2016b) during long-range transport from central Europe (Dall'Osto et al., 2016a). Most single-particle spectra are dominated by either sea salt signatures ($^{23}Na^+$, $^{46}Na_2^+$, $^{62}Na_2O^+$, $^{63}Na_2OH^+$ and $^{81,83}Na_2Cl^+$) (Murphy et al., 2019), by organic fragments (e.g. $^{27}C_2H_3^+$, $^{39}C_3H_3^+$ ~~and $^{39}K^+$~~, $^{43}C_2H_3O^+$ and $^{43}C_3H_7^+$) (Silva and Prather, 2000) or they reveal internal mixtures of these main components. To investigate the Fe-enhancements on the single-particle level and to analyze the role of the particle's main components, we performed a cluster analysis for each set of bipolar single-particle spectra, excluding the mass channels m/z=54…56 that bear potential Fe-signatures. ~~We utilized the adaptive resonance theory neural network, ART-2a~~ (Song et al., 1999) ~~from the open-source toolkit FATES (Flexible Analysis Toolkit for the Exploration of SPMS data)~~ (Sultana et al., 2017). ~~With a learning rate 0.05,~~

~~a vigilance factor of 0.8 and 20 iterations~~, The~~the~~ ART-2a algorithm yielded 149 clusters for the particles ionized with the ArF-laser and 106 clusters for the KrF-laser ionization. Clusters with less than 20 particles were excluded from the analysis. Furthermore, clusters with comparable average mass spectra and the same major ions but slightly varying relative signal intensities were manually merged.

Table 2. Main particle classes from ART-2a clustering and subsequent merging with respect to the major ~~matrix~~ components. The respective mass spectra are shown in Supplemental Figures S62 ~~2~~ and S73 ~~3~~.

	Aged sea salt	Aged sea salt & minor OC	Salt/OC mixed	OC	OC+EC	Fe	Anions only
Dominating ion signals	$^{23}Na^+$, $^{46}Na_2^+$ $^{62}Na_2O^+$, $^{63}Na_2OH^+$, $^{46}NO_2^-$, $^{62}NO_3^-$		$^{23}Na^+$, $^{46}Na_2^+$, $^{39}K^+$ & mol. fragments	$^{39}K^+$, $^{43}C_2H_3O^+$ & molecul. fragments, $^{18}NH_4^+$, $^{30}NO^+$, $^{59}C_3H_9N^+$ (TMA)		$^{56}Fe^+$, $^{73}FeOH^+$	$^{46}NO_2^-$, $^{62}NO_3^-$
Further required signals for assignment	$^{81,83}Na_2Cl^+$, $^{35,37}Cl^-$	$^{39}K^+$ & molecul. fragments	balanced ratio between salt & OC signatures	no or minimal~~um~~ salt signatures	$^{24}C_2^+$, $^{36}C_3^+$, $^{24}C_2^-$, $^{36}C_3^-$,		no cations

The particle ensemble revealed six dominating particle groups, as summarized in Table 2. The corresponding ART-2a area matrices representing the average intensity for each m/z and thus reflecting the typical mass spectra within a group are shown in Supplement Figures S62 and S73. Further separation into subgroups, e.g. with respect to signals from $^{18}NH_4^+$, $^{30}NO^+$ or trimethylamine (TMA, m/z=58…59) (Healy et al., 2015; Köllner et al., 2017) had only limited effects on Fe detection and is consequently not shown here. Mineral dust particles were not observed in appreciable numbers. The measured size distribution is rather narrow, reflecting the instruments optimum ~~detection~~detection efficiency that roughly coincides with the typical size mode undergoing long-range transport, see Supplemental Fig S85.

The particle numbers within the main classes are shown in Fig. 5. There are several differences between the two ionization wavelengths, e.g. the aforementioned overall hit rate. However, here we focus on the detection of Fe. In order to ensure a conservative effect registration (i.e. signals at m/z=56 may also stem from CaO^+ or molecular fragments such as~~like~~ $C_3H_4O^+$) Fe-content is only accounted for particles with a peak area at m/z=56 that is larger than both the signals at m/z=40 (Ca^+) and m/z=55 (principal fragment signal). To further strengthen the screening as recommended by previous studies (Zhang et al., 2014; Dall'Osto et al., 2016a), particles with an additional signal at m/z=54 from the ^{54}Fe isotope, which is lower than 1/10 of the peak area of ^{56}Fe are represented by black bars. Half of the particle spectra that were identified by the algorithm to show the ^{54}Fe isotope, were manually cross-checked on a random basis to prevent false positive results. From the 15,000 particles exposed to the 193 nm laser pulses, less than 100 particles show Fe signatures according to this stringent criterion. As apparent from the enlarged view on the right of Fig. 5(a), nearly all these particles revealed also strong carbon cluster signals from EC. This suggests that they either belong to a particular Fe-rich aerosol class, e.g. from ship emissions or that the EC matrix augments the ionization process of Fe (Zimmermann et al., 2003) in contrast to a salt/OC-matrix, where energetically preferred ions survive collisional charge transfer in the plume (Reinard and Johnston, 2008). Also a suppression of specific ions by the presence of water is conceivable (Neubauer et al., 1998), although a dryer was applied in our experiment. A very different Fe-detection was achieved with the resonant ionization at 248 nm, see Fig. 5(b). Even though the total particle hit rate was lower, many more particles with Fe-signatures were detected. A key finding is that the

Fe-detection is not limited to particles with EC-signatures anymore, but the Fe appears to be internally mixed within particles of several classes. (The relatively low abundance of Fe in the OC-class can be explained by the high contribution of wood/biomass combustion particles.) Remarkably, many particles with low cation signals reveal nearly exclusively Fe-signatures, providing an own group after further classification into subgroups (Fe-signatures were excluded from the first ART-2a clustering).

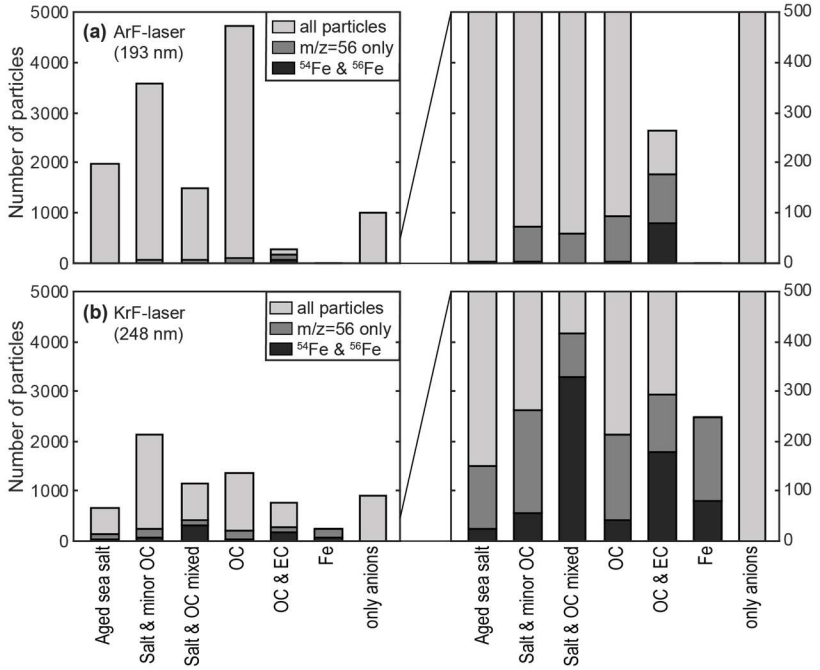

Figure 5. Number of particles within the main classes according to Table 2. Dark grey fractions represent particles with a peak area at m/z=56 being larger than at m/z=55 (molecular fragments) and m/z=40 (Ca^+, because of interference with $^{56}CaO^+$), indicating Fe content. Black fractions illustrate particles showing an additional signal of the less abundant isotope $^{54}Fe^+$. (a) If ionized with 193 nm pulses, substantial fragmentation leads to dominating fragment signals in many of the 15,000 exposed particles. Fe-signals are almost exclusively observed for particles with EC-signatures (see the enlarged view on the right), indicating a particularly high Fe-content or possible interactions with strongly absorbing soot during ionization. (b) Although fewer particles produce ion signals if exposed to 248 nm pulses, the particle fraction showing Fe-signatures is much larger and even a cluster with dominating Fe-signals appears. Of importance, the Fe-signals are not limited to EC-containing particles but can be observed for all classes. This suggests that the resonant ionization ~~is less matrix-dependent and~~ allows a more universal and secure detection of Fe.

Since the same aerosol ensemble was probed with both laser wavelengths, the appearance of Fe-signals for several particle matrices disagrees with the assumption of a particular Fe-rich class. In contrast, different ionization mechanisms are likely to determine the Fe-detection, and resonant LDI appears to feature a more universal and secure detection approach for iron. ~~This is in line with previous studies on REMPI of aromatic substances, showing that resonant ionization (of molecules) in the gaseous plume reduces matrix effects and improves quantification (Woods et al., 2001). Analogously, the reduced effect of the particle matrix renders resonant ionization at the appropriate wavelength a more universal ionization method for metals in SPMS.~~

Although our field study provides only a limited dataset, some general implications can already be derived. The internal mixing of Fe with sulfate or organic acids is assumed to be crucial for Fe dissolution, and thus for the anthropogenic increase of bioavailable iron input to the oceans (Li et al., 2017). Previous studies indicated that the Fe transport into the sea is dominated by coal combustion particles containing sulfate in Asia (Furutani et al., 2011; Moffet et al., 2012), while the majority of Fe-containing particles in Europe are mixed with nitrate and were attributed to traffic activities (Dall'Osto et al., 2016a). Similar to our experiment, these studies found strong internal mixing of many Fe-containing particles, such as biomass burning signals with coal combustion contributions in Asia and secondary nitrate with Fe in Europe. However, Fe-particles with sea-salt signatures were negligible in the SPMS studies and mixtures of Fe and OC were a minor fraction (Furutani et al., 2011; Dall'Osto et al., 2016a). In our study, these particles were the most abundant types of Fe-containing particles, if resonant ionization was applied, see Fig 5(b), while for non-resonant ionization, particles with EC signatures were dominant (Fig. 5(a)). Taking into account that the aforementioned SPMS studies utilized non-resonant LDI of Fe at 266 nm, Fe-transport in organic and salt/mixed aerosols might have been underestimated. Electron microscopy studies of individual particles in Asia frequently revealed thick coatings of secondary compounds and organic matter around Fe-rich particle components (Li et al., 2017; Moffet et al., 2012). Ultra-fine Fe-containing particles, such as soot from traffic emissions, can enter the long-range transported accumulation mode via agglomeration with larger particles and condensation of organic vapours, secondary nitrate or sulfate. In our study, we observed a high prevalence of Fe in sea salt and OC particle types, indicating the importance of these pathways for transport of biologically relevant Fe.

4 Conclusions

In summary, we described enhancements in particle laser desorption/ionization that rely on resonant light absorption by metal atoms. Combining laboratory and field experiments, we showed that the mechanism can be exploited to improve the detection of relevant metals in both natural and anthropogenic aerosols on the single-particle level. Not all physical details are fully understood, and the signal enhancement effects providing the basis for the improved metal detection efficiency are difficult to quantify for the different particle types. However, our results show that the increase in sensitivity is moderate for particular Fe-rich aerosols, such as the about 3-fold signal enhancement for Arizona test dust. The resonance enhancement appears to become more effective for mixed particles with smaller Fe-contributions such as in the ambient air experiment, where about 10 times more particles revealed Fe-signatures in direct comparison with non-resonant ionization. Taking into account the lower hit rate of the KrF laser that is related to its lower photon energy, the overall efficiency to identify Fe signatures in a single-particle mass spectrum was increased by a factor of about 20 in our ambient air study.

The coincidental matching of the KrF laser line with a strong absorption of Fe atoms allows an easy and straightforward application of the resonance effect in the field. For direct comparison of KrF with ArF lasers, it has to be considered that the lower photon energy of KrF laser is associated with a reduced hit rate and different mass spectral signatures of other particle components, e.g. organics. Further studies are required to evaluate these differences. Of note, because of its rather high

pulse energy and the flat-top beam profile, the hit rate of the KrF laser was about 40−50 % in our experiment, which is still more than the values that are typically achieved with the most common laser line in SPMS, the Nd:YAG at 266 nm. Exploiting the resonance effect for other metals than Fe requires a tuneable Nd:YAG-OPO system, which is, however, more difficult to operate.

With the improved detection of Fe and its inherent sensitivity to further key nutrients such as nitrate and phosphate, SPMS becomes an interesting complement to established methods for investigating atmospheric Fe transport. Moreover, several key parameters for the metal's bioavailability, including the particle size or the presence of carboxylic acids and sulfate (Fang et al., 2017) can be determined on a single-particle level. Because of the high time resolution, SPMS-based Fe detection may be particularly helpful for studies on the oceans' rapid response to the naturally episodic depositions of Fe and other micronutrients. Beyond these direct applications, more studies are required to elucidate the promising implications for SPMS quantification approaches (Healy et al., 2013; Gemayel et al., 2017). Of note, the Fe-containing particles can further be characterized with regard to their organic content using multi-step ionization techniques (Schade et al., 2019; Czech et al., 2017). This is of importance for health-related studies, as two of the most relevant adverse aerosol compounds, transition metals and PAHs, can be addressed with the same, easily accessible KrF-excimer laser wavelength. Such hyphenated single-particle schemes bear great potential to elucidate intriguing interactions in atmospheric heterogeneous and multiphase chemistry (Pöschl and Shiraiwa, 2015), for example with regard to possible catalytic activities of the in particle's metal content (Sullivan et al., 2007). In conclusion, the described resonance effects pave a new route towards improved detection of air pollutants and a more profound understanding of the aerosol impact on biogeochemical cycles and human health.

Data availability

Data are available on request from Johannes Passig (johannes.passig@uni-rostock.de).

Author Contributions

J.P. and J.S. contributed equally to this work. J.P. conceived the experiments. J.S., E.-I.R. J.P., T.K.-B. and R.I. performed the experiments. L.L., X.L. and Z.Z. provided the SPMS instrument as well as technical support. T.K.-B. developed the electronics. H.C., M.S., T.S. and R.Z. provided assistance with data interpretation. J.M. and H.F. hosted and supported the field study. J.S., J.P. and E.-I.R. analyzed data and prepared the figures. J.P. wrote the manuscript with contributions from all authors.

Competing interests

The authors declare that they have no conflict of interest.

Acknowledgements

We thank Johan Mellqvist, John Conway, Lars Eriksson and co-workers from the Chalmers University of Technology and from the IVL Miljöinstitut for hosting the field experiments and their support.

The Project was funded by the German Research Foundation (ZI 764/6-1), by the German Federal Ministry for Economic Affairs and Energy (ZF4402101 ZG7), by the Helmholtz International Lab aeroHEALTH (www.aerohealth.eu) and by the Helmholtz Virtual Institute of Complex Molecular Systems in Environmental Health (www.hice-vi.eu).

References

Arndt, J., Sciare, J., Mallet, M., Roberts, G. C., Marchand, N., Sartelet, K., Sellegri, K., Dulac, F., Healy, R. M., and Wenger, J. C.: Sources and mixing state of summertime background aerosol in the north-western Mediterranean basin, Atmos. Chem. Phys., 17, 6975–7001, doi:10.5194/acp-17-6975-2017, 2017.

Ault, A. P., Gaston, C. I., Wang, Y., Dominguez, G., Thiemens, M. H., and Prather, K. A.: Characterization of the single particle mixing state of individual ship plume events measured at the Port of Los Angeles, Environ. Sci. Technol., 44, 1954–1961, doi:10.1021/es902985h, 2010.

Bente, M., Sklorz, M., Streibel, T., and Zimmermann, R.: Online laser desorption-multiphoton postionization mass spectrometry of individual aerosol particles: molecular source indicators for particles emitted from different traffic-related and wood combustion sources, Anal. Chem., 80, 8991–9004, doi:10.1021/ac801295f, 2008.

Bente, M., Sklorz, M., Streibel, T., and Zimmermann, R.: Thermal desorption-multiphoton ionization time-of-flight mass spectrometry of individual aerosol particles: a simplified approach for online single-particle analysis of polycyclic aromatic hydrocarbons and their derivatives, Anal. Chem., 81, 2525–2536, doi:10.1021/ac802296f, 2009.

Bond, T. C., Doherty, S. J., Fahey, D. W., Forster, P. M., Berntsen, T., DeAngelo, B. J., Flanner, M. G., Ghan, S., Kärcher, B., Koch, D., Kinne, S., Kondo, Y., Quinn, P. K., Sarofim, M. C., Schultz, M. G., Schulz, M., Venkataraman, C., Zhang, H., Zhang, S., Bellouin, N., Guttikunda, S. K., Hopke, P. K., Jacobson, M. Z., Kaiser, J. W., Klimont, Z., Lohmann, U., Schwarz, J. P., Shindell, D., Storelvmo, T., Warren, S. G., and Zender, C. S.: Bounding the role of black carbon in the climate system: A scientific assessment, J. Geophys. Res., 118, 5380–5552, doi:10.1002/jgrd.50171, 2013.

Boyd, P. W., Ellwood, M. J., Tagliabue, A., and Twining, B. S.: Biotic and abiotic retention, recycling and remineralization of metals in the ocean, Nature Geosci, 10, 167–173, doi:10.1038/ngeo2876, 2017.

Carson, P. G., Johnston, M. V., and Wexler, A. S.: Real-Time Monitoring of the Surface and Total Composition of Aerosol Particles, Aerosol Sci. Technol., 26, 291–300, doi:10.1080/02786829708965431, 1997.

Conway, T. M., Hamilton, D. S., Shelley, R. U., Aguilar-Islas, A. M., Landing, W. M., Mahowald, N. M., and John, S. G.: Tracing and constraining anthropogenic aerosol iron fluxes to the North Atlantic Ocean using iron isotopes, Nat. Commun., 10, 1–10, doi:10.1038/s41467-019-10457-w, 2019.

Czech, H., Stengel, B., Adam, T., Sklorz, M., Streibel, T., and Zimmermann, R.: A chemometric investigation of aromatic emission profiles from a marine engine in comparison with residential wood combustion and road traffic: Implications for source apportionment inside and outside sulphur emission control areas, Atmospheric Environ., 167, 212–222, doi:10.1016/j.atmosenv.2017.08.022, 2017.

Dall'Osto, M., Harrison, R. M., Highwood, E. J., O'Dowd, C., Ceburnis, D., Querol, X., and Achterberg, E. P.: Variation of the mixing state of Saharan dust particles with atmospheric transport, Atmospheric Environ., 44, 3135–3146, doi:10.1016/j.atmosenv.2010.05.030, 2010.

Dall'Osto, M., Beddows, D. C. S., Harrison, R. M., and Onat, B.: Fine Iron Aerosols Are Internally Mixed with Nitrate in the Urban European Atmosphere, Environ. Sci. Technol., 50, 4212–4220, doi:10.1021/acs.est.6b01127, 2016a.

Dall'Osto, M., Beddows, D. C. S., McGillicuddy, E. J., Esser-Gietl, J. K., Harrison, R. M., and Wenger, J. C.: On the simultaneous deployment of two single-particle mass spectrometers at an urban background and a roadside site during SAPUSS, Atmospheric Chemistry and Physics, 16, 9693–9710, doi:10.5194/acp-16-9693-2016, 2016b.

Fang, T., Guo, H., Zeng, L., Verma, V., Nenes, A., and Weber, R. J.: Highly Acidic Ambient Particles, Soluble Metals, and Oxidative Potential: A Link between Sulfate and Aerosol Toxicity, Environ. Sci. Technol., 51, 2611–2620, doi:10.1021/acs.est.6b06151, 2017.

Fergenson, D. P., Song, X. H., Ramadan, Z., Allen, J. O., Hughes, L. S., Cass, G. R., Hopke, P. K., and Prather, K. A.: Quantification of ATOFMS data by multivariate methods, Anal. Chem., 73, 3535–3541, doi:10.1021/ac010022j, 2001.

Furutani, H., Jung, J., Miura, K., Takami, A., Kato, S., Kajii, Y., and Uematsu, M.: Single-particle chemical characterization and source apportionment of iron-containing atmospheric aerosols in Asian outflow, J. Geophys. Res., 116, 5504, doi:10.1029/2011JD015867, 2011.

Gard, Kleeman, Gross, Hughes, Allen, Morrical, Fergenson, Dienes, E Galli, M., Johnson, Cass, and Prather: Direct observation of heterogeneous chemistry in the atmosphere, Science, 279, 1184–1187, doi:10.1126/science.279.5354.1184, 1998.

Gaur, S. and Agnihotri, R.: Health Effects of Trace Metals in Electronic Cigarette Aerosols-a Systematic Review, Biological trace element research, 188, 295–315, doi:10.1007/s12011-018-1423-x, 2019.

Gemayel, R., Temime-Roussel, B., Hayeck, N., Gandolfo, A., Hellebust, S., Gligorovski, S., and Wortham, H.: Development of an analytical methodology for obtaining quantitative mass concentrations from LAAP-ToF-MS measurements, Talanta, 174, 715–724, doi:10.1016/j.talanta.2017.06.050, 2017.

Gonzalez, C. A. and Choquette, S. J.: Certificate of Analysis: Standard Reference Material 1649b: https://www-s.nist.gov/srmors/certificates/1649b.pdf, last access: 23 April 2020.

Gross, D. S., Gälli, M. E., Silva, P. J., and Prather, K. A.: Relative Sensitivity Factors for Alkali Metal and Ammonium Cations in Single-Particle Aerosol Time-of-Flight Mass Spectra, Anal. Chem., 72, 416–422, doi:10.1021/ac990434g, 2000.

Gunzer, F., Krüger, S., and Grotemeyer, J.: Photoionization and photofragmentation in mass spectrometry with visible and UV lasers, Mass Spectrom. Rev., 38, 202–217, doi:10.1002/mas.21579, 2019.

Hatch, L. E., Pratt, K. A., Huffman, J. A., Jimenez, J. L., and Prather, K. A.: Impacts of Aerosol Aging on Laser Desorption/Ionization in Single-Particle Mass Spectrometers, Aerosol Sci. Technol., 48, 1050–1058, doi:10.1080/02786826.2014.955907, 2014.

Healy, R. M., Evans, G. J., Murphy, M., Sierau, B., Arndt, J., McGillicuddy, E., O'Connor, I. P., Sodeau, J. R., and Wenger, J. C.: Single-particle speciation of alkylamines in ambient aerosol at five European sites, Analytical and bioanalytical chemistry, 407, 5899–5909, doi:10.1007/s00216-014-8092-1, 2015.

Healy, R. M., O'Connor, I. P., Hellebust, S., Allanic, A., Sodeau, J. R., and Wenger, J. C.: Characterisation of single particles from in-port ship emissions, Atmospheric Environ., 43, 6408–6414, doi:10.1016/j.atmosenv.2009.07.039, 2009.

Healy, R. M., Sciare, J., Poulain, L., Crippa, M., Wiedensohler, A., Prévôt, A. S. H., Baltensperger, U., Sarda-Estève, R., McGuire, M. L., Jeong, C.-H., McGillicuddy, E., O&apos, Connor, I. P., Sodeau, J. R., Evans, G. J., and Wenger, J. C.: Quantitative determination of carbonaceous particle mixing state in Paris using single-particle mass spectrometer and aerosol mass spectrometer measurements, Atmos. Chem. Phys., 13, 9479–9496, doi:10.5194/acp-13-9479-2013, 2013.

Hinz, K.-P. and Spengler, B.: Instrumentation, data evaluation and quantification in on-line aerosol mass spectrometry, Journal of mass spectrometry JMS, 42, 843–860, doi:10.1002/jms.1262, 2007.

Hübert, W. and Ankerhold, G.: Elemental misinterpretation in automated analysis of LIBS spectra, Analytical and bioanalytical chemistry, 400, 3273–3278, doi:10.1007/s00216-011-4793-x, 2011.

Ito, A.: Atmospheric Processing of Combustion Aerosols as a Source of Bioavailable Iron, Environ. Sci. Technol. Lett., 2, 70–75, doi:10.1021/acs.estlett.5b00007, 2015.

Ito, A. and Shi, Z.: Delivery of anthropogenic bioavailable iron from mineral dust and combustion aerosols to the ocean, Atmos. Chem. Phys., 16, 85–99, doi:10.5194/acp-16-85-2016, 2016.

Jickells, T. D., An, Z. S., Andersen, K. K., Baker, A. R., Bergametti, G., Brooks, N., Cao, J. J., Boyd, P. W., Duce, R. A., Hunter, K. A., Kawahata, H., Kubilay, N., laRoche, J., Liss, P. S., Mahowald, N., Prospero, J. M., Ridgwell, A. J., Tegen, I., and Torres, R.: Global iron connections between desert dust, ocean biogeochemistry, and climate, Science, 308, 67–71, doi:10.1126/science.1105959, 2005.

Kanakidou, M., Seinfeld, J. H., Pandis, S. N., Barnes, I., Dentener, F. J., Facchini, M. C., van Dingenen, R., Ervens, B., Nenes, A., Nielsen, C. J., Swietlicki, E., Putaud, J. P., Balkanski, Y., Fuzzi, S., Horth, J., Moortgat, G. K., Winterhalter, R., Myhre, C. E. L., Tsigaridis, K., Vignati, E., Stephanou, E. G., and Wilson, J.: Organic aerosol and global climate modelling: a review, Atmos. Chem. Phys., 5, 1053–1123, doi:10.5194/acp-5-1053-2005, 2005.

Kanashova, T., Sippula, O., Oeder, S., Streibel, T., Passig, J., Czech, H., Kaoma, T., Sapcariu, S. C., Dilger, M., Paur, H.-R., Schlager, C., Mülhopt, S., Weiss, C., Schmidt-Weber, C., Traidl-Hoffmann, C., Michalke, B., Krebs, T., Karg, E., Jakobi, G., Scholtes, S., Schnelle-Kreis, J., Sklorz, M., Orasche, J., Müller, L., Reda, A., Rüger, C., Neumann, A., Abbaszade, G., Radischat, C., Hiller, K., Grigonyte, J., Kortelainen, M., Kuuspalo, K., Lamberg, H., Leskinen, J., Nuutinen, I., Torvela, T., Tissari, J., Jalava, P., Kasurinen, S., Uski, O., Hirvonen, M.-R., Buters, J., Dittmar, G., Jokiniemi, J. K., and Zimmermann, R.: Emissions from a modern log wood masonry heater and wood pellet boiler Composition and biological impact on air-liquid interface exposed human lung cancer cells, Journal of Molecular and Clinical Medicine, 1, 23, doi:10.31083/j.jmcm.2018.01.004, 2018.

Köllner, F., Schneider, J., Willis, M. D., Klimach, T., Helleis, F., Bozem, H., Kunkel, D., Hoor, P., Burkart, J., Leaitch, W. R., Aliabadi, A. A., Abbatt, J. P. D., Herber, A. B., and Borrmann, S.: Particulate trimethylamine in the summertime Canadian high Arctic lower troposphere, Atmos. Chem. Phys., 17, 13747–13766, doi:10.5194/acp-17-13747-2017, 2017.

Kramida, A. and Ralchenko, Y.: NIST Atomic Spectra Database, NIST Standard Reference Database 78.

Laskin, J., Laskin, A., and Nizkorodov, S. A.: Mass Spectrometry Analysis in Atmospheric Chemistry, Anal. Chem., 90, 166–189, doi:10.1021/acs.analchem.7b04249, 2018.

Li, C., He, Q., Schade, J., Passig, J., Zimmermann, R., Meidan, D., Laskin, A., and Rudich, Y.: Dynamic changes in optical and chemical properties of tar ball aerosols by atmospheric photochemical aging, Atmos. Chem. Phys., 19, 139–163, doi:10.5194/acp-19-139-2019, 2019.

Li, L., Huang, Z., Dong, J., Li, M., Gao, W., Nian, H., Fu, Z., Zhang, G., Bi, X., Cheng, P., and Zhou, Z.: Real time bipolar time-of-flight mass spectrometer for analyzing single aerosol particles, Int. J. Mass Spectrom., 303, 118–124, doi:10.1016/j.ijms.2011.01.017, 2011.

Li, L., Liu, L., Xu, L., Li, M., Li, X., Gao, W., Huang, Z., and Cheng, P.: Improvement in the Mass Resolution of Single Particle Mass Spectrometry Using Delayed Ion Extraction, J. Am. Soc. Mass Spectrom., 29, 2105–2109, doi:10.1007/s13361-018-2037-4, 2018.

Li, W., Xu, L., Liu, X., Zhang, J., Lin, Y., Yao, X., Gao, H., Zhang, D., Chen, J., Wang, W., Harrison, R. M., Zhang, X., Shao, L., Fu, P., Nenes, A., and Shi, Z.: Air pollution-aerosol interactions produce more bioavailable iron for ocean ecosystems, Sci. Adv., 3, e1601749, doi:10.1126/sciadv.1601749, 2017.

Mahowald, N. M., Hamilton, D. S., Mackey, K. R. M., Moore, J. K., Baker, A. R., Scanza, R. A., and Zhang, Y.: Aerosol trace metal leaching and impacts on marine microorganisms, Nat. Commun., 9, 2614, doi:10.1038/s41467-018-04970-7, 2018.

McLean, C. J., Marsh, J. H., Land, A. P., Clark, A., Jennings, R., Ledingham, K.W.D., McCombes, P. T., Marshall, A., Singhal, R. P., and Towrie, M.: Resonant laser ablation (RLA), Int. J. Mass Spectrom., 96, R1-R7, doi:10.1016/0168-1176(90)80047-7, 1990.

Moffet, R. C., Furutani, H., Rödel, T. C., Henn, T. R., Sprau, P. O., Laskin, A., Uematsu, M., and Gilles, M. K.: Iron speciation and mixing in single aerosol particles from the Asian continental outflow, J. Geophys. Res., 117, n/a-n/a, doi:10.1029/2011JD016746, 2012.

Morrical, B. D., Fergenson, D. P., and Prather, K. A.: Coupling two-step laser desorption/ionization with aerosol time-of-flight mass spectrometry for the analysis of individual organic particles, J. Am. Soc. Mass Spectrom., 9, 1068–1073, doi:10.1016/S1044-0305(98)00074-9, 1998.

Murphy, D. M.: The design of single particle laser mass spectrometers, Mass Spectrom. Rev., 26, 150–165, doi:10.1002/mas.20113, 2007.

Murphy, D. M., Froyd, K. D., Bian, H., Brock, C. A., Dibb, J. E., DiGangi, J. P., Diskin, G., Dollner, M., Kupc, A., Scheuer, E. M., Schill, G. P., Weinzierl, B., Williamson, C. J., and Yu, P.: The distribution of sea-salt aerosol in the global troposphere, Atmos. Chem. Phys., 19, 4093–4104, doi:10.5194/acp-19-4093-2019, 2019.

Neubauer, K. R., Johnston, M. V., and Wexler, A. S.: Humidity effects on the mass spectra of single aerosol particles, Atmospheric Environ., 32, 2521–2529, doi:10.1016/S1352-2310(98)00005-3, 1998.

Oakes, M., Ingall, E. D., Lai, B., Shafer, M. M., Hays, M. D., Liu, Z. G., Russell, A. G., and Weber, R. J.: Iron solubility related to particle sulfur content in source emission and ambient fine particles, Environ. Sci. Technol., 46, 6637–6644, doi:10.1021/es300701c, 2012.

Passig, J., Schade, J., Oster, M., Fuchs, M., Ehlert, S., Jäger, C., Sklorz, M., and Zimmermann, R.: Aerosol Mass Spectrometer for Simultaneous Detection of Polyaromatic Hydrocarbons and Inorganic Components from Individual Particles, Anal. Chem., 89, 6341–6345, doi:10.1021/acs.analchem.7b01207, 2017.

Pöschl, U. and Shiraiwa, M.: Multiphase chemistry at the atmosphere-biosphere interface influencing climate and public health in the anthropocene, Chem. Rev., 115, 4440–4475, doi:10.1021/cr500487s, 2015.

Pratt, K. A., Mayer, J. E., Holecek, J. C., Moffet, R. C., Sanchez, R. O., Rebotier, T. P., Furutani, H., Gonin, M., Fuhrer, K., Su, Y., Guazzotti, S., and Prather, K. A.: Development and characterization of an aircraft aerosol time-of-flight mass spectrometer, Anal. Chem., 81, 1792–1800, doi:10.1021/ac801942r, 2009.

Pratt, K. A. and Prather, K. A.: Mass spectrometry of atmospheric aerosols--recent developments and applications. Part II: On-line mass spectrometry techniques, Mass Spectrom. Rev., 31, 17–48, doi:10.1002/mas.20330, 2012.

Qin, X., Bhave, P. V., and Prather, K. A.: Comparison of two methods for obtaining quantitative mass concentrations from aerosol time-of-flight mass spectrometry measurements, Anal. Chem., 78, 6169–6178, doi:10.1021/ac060395q, 2006.

Reilly, P. T. A., Lazar, A. C., Gieray, R. A., Whitten, W. B., and Ramsey, J. M.: The Elucidation of Charge-Transfer-Induced Matrix Effects in Environmental Aerosols Via Real-Time Aerosol Mass Spectral Analysis of Individual Airborne Particles, Aerosol Sci. Technol., 33, 135–152, doi:10.1080/027868200410895, 2000.

Reinard, M. S. and Johnston, M. V.: Ion formation mechanism in laser desorption ionization of individual nanoparticles, J. Am. Soc. Mass Spectrom., 19, 389–399, doi:10.1016/j.jasms.2007.11.017, 2008.

Schade, J., Passig, J., Irsig, R., Ehlert, S., Sklorz, M., Adam, T., Li, C., Rudich, Y., and Zimmermann, R.: Spatially Shaped Laser Pulses for the Simultaneous Detection of Polycyclic Aromatic Hydrocarbons as well as Positive and Negative Inorganic Ions in Single Particle Mass Spectrometry, Anal. Chem., 91, 10282–10288, doi:10.1021/acs.analchem.9b02477, 2019.

Schoolcraft, T. A., Constable, G. S., Zhigilei, L. V., and Garrison, B. J.: Molecular dynamics simulation of the laser disintegration of aerosol particles, Anal. Chem., 72, 5143–5150, doi:10.1021/ac0007635, 2000.

Seder, T. A., Ouderkirk, A. J., and Weitz, E.: The wavelength dependence of excimer laser photolysis of Fe(CO) 5 in the gas phase. Transient infrared spectroscopy and kinetics of the Fe(CO) x (x =4,3,2) photofragments, J. Chem. Phys., 85, 1977–1986, doi:10.1063/1.451141, 1986.

Seinfeld, J. H. and Pandis, S. N.: Atmospheric chemistry and physics: From air pollution to climate change, 3rd edition, Wiley, Hoboken, New Jersey, 1120 pp., 2016.

Shen, X., Saathoff, H., Huang, W., Mohr, C., Ramisetty, R., and Leisner, T.: Understanding atmospheric aerosol particles with improved particle identification and quantification by single-particle mass spectrometry, Atmos. Meas. Tech., 12, 2219–2240, doi:10.5194/amt-12-2219-2019, 2019.

Silva, P. J. and Prather, K. A.: Interpretation of Mass Spectra from Organic Compounds in Aerosol Time-of-Flight Mass Spectrometry, Anal. Chem., 72, 3553–3562, doi:10.1021/ac9910132, 2000.

Sofiev, M., Winebrake, J. J., Johansson, L., Carr, E. W., Prank, M., Soares, J., Vira, J., Kouznetsov, R., Jalkanen, J.-P., and Corbett, J. J.: Cleaner fuels for ships provide public health benefits with climate tradeoffs, Nat. Commun., 9, 406, doi:10.1038/s41467-017-02774-9, 2018.

Song, X.-H., Hopke, P. K., Fergenson, D. P., and Prather, K. A.: Classification of Single Particles Analyzed by ATOFMS Using an Artificial Neural Network, ART-2A, Anal. Chem., 71, 860–865, doi:10.1021/ac9809682, 1999.

Su, Y., Sipin, M. F., Furutani, H., and Prather, K. A.: Development and characterization of an aerosol time-of-flight mass spectrometer with increased detection efficiency, Analytical chemistry, 76, 712–719, doi:10.1021/ac034797z, 2004.

Sullivan, R. C., Guazzotti, S. A., Sodeman, D. A., and Prather, K. A.: Direct observations of the atmospheric processing of Asian mineral dust, Atmos. Chem. Phys., 7, 1213–1236, doi:10.5194/acp-7-1213-2007, 2007.

Sultana, C. M., Cornwell, G. C., Rodriguez, P., and Prather, K. A.: FATES: a flexible analysis toolkit for the exploration of single-particle mass spectrometer data, Atmos. Meas. Tech., 10, 1323–1334, doi:10.5194/amt-10-1323-2017, 2017.

Thomson, D. S., Middlebrook, A. M., and Murphy, D. M.: Thresholds for Laser-Induced Ion Formation from Aerosols in a Vacuum Using Ultraviolet and Vacuum-Ultraviolet Laser Wavelengths, Aerosol Sci. Technol., 26, 544–559, doi:10.1080/02786829708965452, 1997.

Toner, S. M., Sodeman, D. A., and Prather, K. A.: Single Particle Characterization of Ultrafine and Accumulation Mode Particles from Heavy Duty Diesel Vehicles Using Aerosol Time-of-Flight Mass Spectrometry, Environ. Sci. Technol., 40, 3912–3921, doi:10.1021/es051455x, 2006.

Trainor, D. W. and Mani, S. A.: Pumping iron: A KrF laser pumped atomic iron laser, J. Chem. Phys., 68, 5481–5485, doi:10.1063/1.435727, 1978.

Uski, O., Jalava, P. I., Happo, M. S., Torvela, T., Leskinen, J., Mäki-Paakkanen, J., Tissari, J., Sippula, O., Lamberg, H., Jokiniemi, J., and Hirvonen, M.-R.: Effect of fuel zinc content on toxicological responses of particulate matter from pellet combustion in vitro, Sci. Total Environ., 511, 331–340, doi:10.1016/j.scitotenv.2014.12.061, 2015.

Vera, C. C., Trimborn, A., Hinz, K.-P., and Spengler, B.: Initial velocity distributions of ions generated by in-flight laser desorption/ionization of individual polystyrene latex microparticles as studied by the delayed ion extraction method, Rapid Commun. Mass Spectrom., 19, 133–146, doi:10.1002/rcm.1753, 2005.

Verdun, F. R., Krier, G., and Muller, J. F.: Increased sensitivity in laser microprobe mass analysis by using resonant two-photon ionization processes, Anal. Chem., 59, 1383–1387, doi:10.1021/ac00137a003, 1987.

Wade, E. E., Farquar, G. R., Steele, P. T., McJimpsey, E. L., Lebrilla, C. B., and Fergenson, D. P.: Wavelength and size dependence in single particle laser aerosol mass spectra, J. Aerosol Sci., 39, 657–666, doi:10.1016/j.jaerosci.2008.03.007, 2008.

Wang, G., Zhang, R., Gomez, M. E., Yang, L., Levy Zamora, M., Hu, M., Lin, Y., Peng, J., Guo, S., Meng, J., Li, J., Cheng, C., Hu, T., Ren, Y., Wang, Y., Gao, J., Cao, J., An, Z., Zhou, W., Li, G., Wang, J., Tian, P., Marrero-Ortiz, W., Secrest, J., Du, Z., Zheng, J., Shang, D., Zeng, L., Shao, M., Wang, W., Huang, Y., Wang, Y., Zhu, Y., Li, Y., Hu, J., Pan, B., Cai, L., Cheng, Y., Ji, Y., Zhang, F., Rosenfeld, D., Liss, P. S., Duce, R. A., Kolb, C. E., and Molina, M. J.: Persistent sulfate formation from London Fog to Chinese haze, Proc. Natl. Acad. Sci. USA, 113, 13630–13635, doi:10.1073/pnas.1616540113, 2016.

Woods, E., Smith, G. D., Dessiaterik, Y., Baer, T., and Miller, R. E.: Quantitative Detection of Aromatic Compounds in Single Aerosol Particle Mass Spectrometry, Anal. Chem., 73, 2317–2322, doi:10.1021/ac001166l, 2001.

Ye, D., Klein, M., Mulholland, J. A., Russell, A. G., Weber, R., Edgerton, E. S., Chang, H. H., Sarnat, J. A., Tolbert, P. E., and Ebelt Sarnat, S.: Estimating Acute Cardiovascular Effects of Ambient PM2.5 Metals, Environ. Health Perspect., 126, 27007, doi:10.1289/EHP2182, 2018.

Young, J. P., Shaw, R. W., and Smith, D. H.: Resonance ionization mass spectrometry, Anal. Chem., 61, 1271A-1279A, doi:10.1021/ac00197a002, 1989.

Zhang, G., Bi, X., Lou, S., Li, L., Wang, H., Wang, X., Zhou, Z., Sheng, G., Fu, J., and Chen, C.: Source and mixing state of iron-containing particles in Shanghai by individual particle analysis, Chemosphere, 95, 9–16, doi:10.1016/j.chemosphere.2013.04.046, 2014.

Zhou, Y., Huang, X. H., Griffith, S. M., Li, M., Li, L., Zhou, Z., Wu, C., Meng, J., Chan, C. K., Louie, P. K.K., and Yu, J. Z.: A field measurement based scaling approach for quantification of major ions, organic carbon, and elemental carbon using a single particle aerosol mass spectrometer, Atmospheric Environ., 143, 300–312, doi:10.1016/j.atmosenv.2016.08.054, 2016.

Zimmermann, R., Ferge, T., Gälli, M., and Karlsson, R.: Application of single-particle laser desorption/ionization time-of-flight mass spectrometry for detection of polycyclic aromatic hydrocarbons from soot particles originating from an industrial combustion process, Rapid Commun. Mass Spectrom., 17, 851–859, doi:10.1002/rcm.979, 2003.